AD-762 531

REFRACTORY CHAMBER MATERIALS FOR N$_2$O$_4$/AMINE PROPELLANTS

John G. Campbell

Marquardt Company
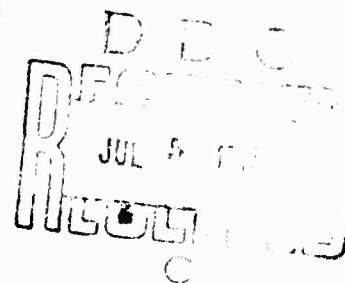
Prepared for:

Air Force Rocket Propulsion Laboratory

May 1973

AD 762531

REFRACTORY CHAMBER MATERIALS
FOR
N₂O₄/AMINE PROPELLANTS

J. G. Campbell

THE MARQUARDT COMPANY
VAN NUYS, CALIFORNIA

APPROVED FOR PUBLIC RELEASE; DISTRIBUTION UNLIMITED

NOTICES

"When US Government drawings, specifications, or other data are
used for any purpose other than a definitely related Government procurement
operation, the Government thereby incurs no responsibility nor any obligation
whatsoever, and the fact that the Government may have formulated, furnished,
or in any way supplied the said drawings, specifications or other data, is not
to be regarded by implication or otherwise, or in any manner licensing the
holder or any other person or corporation, or conveying any rights or per-
mission to manufacture, use, or sell any patented invention that may in any
way be related thereto. "

DISCLAIMER NOTICE

DEFENSE TECHNICAL INFORMATION CENTER

THIS DOCUMENT IS BEST QUALITY AVAILABLE. THE COPY FURNISHED TO DTIC CONTAINED A SIGNIFICANT NUMBER OF PAGES WHICH DO NOT REPRODUCE LEGIBLY.

DOCUMENT CONTROL DATA - R & D

(Security classification of title, body of abstract and indexing annotation must be entered when the overall report is classified)

1 ORIGINATING ACTIVITY (Corporate author)	2a. REPORT SECURITY CLASSIFICATION
The Marquardt Company	UNCLASSIFIED
16555 Saticoy Street	2b GROUP
Van Nuys, California 91409	

3 REPORT TITLE

Refractory Chamber Materials for N_2O_4/Amine Propellants

4 DESCRIPTIVE NOTES (Type of report and inclusive dates)

5 AUTHOR(S) (First name, middle initial, last name)

John G. Campbell

6 REPORT DATE	7a. TOTAL NO OF PAGES	7b. NO OF REFS
May 1973	75 83	9
8a. CONTRACT OR GRANT NO	9a. ORIGINATOR'S REPORT NUMBER(S)	
F04611-71-C-0007	Marquardt Report S-1250	
b. PROJECT NO		
3058		
c.	9b. OTHER REPORT NO(S) (Any other numbers that may be assigned this report)	
d.	AFRPL-TR-73-31	

10 DISTRIBUTION STATEMENT

Approved for Public Release, Distribution Unlimited

11 SUPPLEMENTARY NOTES	12. SPONSORING MILITARY ACTIVITY
	Air Force Rocket Propulsion Laboratory
	Edwards Air Force Base, California 93523

13. ABSTRACT

Oxidation resistant materials suitable for passively cooled thrust chambers for N_2O_4 Amine propellants were evaluated by nozzle test firings at 400 psia to 600 psia.

Thermal stress analysis was performed to establish designs capable of performing long duration, multiple restart duty cycles. A nozzle insert made of edge oriented washers of zirconium pyrocarbide and hafnium pyrocarbide experienced high erosion rates comparable to pyrolytic graphite washers. A pyrolytic graphite coated Carbitex nozzle experienced low erosion rates, about 1 mil/sec. The best erosion resistance was demonstrated by a zirconium diboride insert made of Material VIII (18, 10) from Man Labs, Inc. This insert, in the form of two segments, was designed to resist thermal shock by free thermal expansion and by heat flux reduction through a preoxidized coating. This nozzle concept allows the use of materials formerly prohibited from rocket nozzle applications because of thermal stress sensitivity.

DD ⁣ FORM ⁣ NOV 65 ⁣ 1473

14 KEY WORDS	LINK A		LINK B		LINK C	
	ROLE	WT	ROLE	WT	ROLE	WT
Rocket Nozzles						
Refractory Materials						
Pyrolytic Graphite						
Borides						
Carbides						

1 - a

FOREWORD

This is the final report submitted in fulfillment of Contract F04611-71-C-007 with the Air Force Rocket Propulsion Laboratory. The Air Force Project Engineer was Capt. Phil Martin.

The contract effort was conducted by the Marquardt Engineering Division under J. G. Campbell, Program Manager. Participants at Marquardt included M. S. Wilson, Thermal Analysis and R. V. Loustau, Design. A subcontract performed by the Raytheon Company, Waltham, Mass. was managed by Dr. S. Waugh. Mr. R. Grossman acted as consultant for Man Labs, Inc.

The report (Marquardt No. S-1250) has been prepared in accordance with MIL-STD-847 (USAF) dated 25 February 1965. The period of activity was October 1970 through February 1973.

This technical report has been reviewed and is approved.

Charles E. Sieber, Lt. Col. USAF
Chief, Liquid Rocket Division
AFRPL

ABSTRACT

Oxidation resistant materials suitable for passively cooled thrust chambers for N_2O_4/Amine propellants were evaluated by nozzle test firings at 400 psia to 600 psia.

Thermal stress analysis was performed to establish designs capable of performing for long duration, multiple restart duty cycles. A nozzle insert made of edge oriented washers of zirconium pyrocarbide and hafnium pyrocarbide experienced high erosion rates comparable to pyrolytic graphite washers. A pyrolytic graphite coated Carbitex nozzle experienced low erosion rates, about .6mil/sec. The best erosion resistance was demonstrated by a zirconium diboride insert made of Material VIII (18, 10) from Man Labs, Inc. This insert, in the form of two segments, was designed to resist thermal shock by free thermal expansion and by heat flux reduction through a preoxidized coating. This nozzle concept allows the use of materials formerly prohibited from rocket nozzle applications because of thermal stress sensitivity.

TABLE OF CONTENTS

Preceding page blank

LIST OF ILLUSTRATIONS

SECTION I

INTRODUCTION

This report presents the results of a program conducted by The Marquardt Company to evaluate oxidation resistant materials for application to passively cooled thrust chambers for N_2O_4/Amine propellant combinations at chamber pressures from 400 psia to 600 psia. Three types of high temperature materials were tested in nozzle firings at AFRPL, Edwards, California. The three types of materials tested were as follows:

- Zirconium diboride alloys
- Pyrolytic Graphite
- Zirconium Pyrocarbide and Hafnium Pyrocarbide.

The material which demonstrated the best erosion and oxidation resistance was a zirconium diboride alloy, Man Labs Material VIII (18, 10), containing eighteen percent SiC and ten percent graphite. The successful demonstration of this material was due to development of a new design concept for thermal shock resistant rocket nozzles.

Segments of a zirconium diboride alloy were designed by Marquardt to resist thermal shock by free thermal expansion. Pyrolytic graphite springs surrounding the throat segments provided a unique method of holding the segments in position under handling and vibration, while also allowing thermal expansion of the segments during engine firing.

The thermal stresses in the segments were also reduced by a coating of low thermal conductivity oxides formed by pre-oxidation. The pre-oxidized coating adhered to the segments during engine firings at 400 psia. No thermal stress cracking or measurable erosion was encountered during a 25 second firing with the oxidizing propellants N_2O_4/N_2H_4. A second run of 53 seconds was also made with minimal erosion of the nozzle segments, although one of the pyrolytic graphite springs was displaced, reducing thermal expansion and causing several cracks in the boride inserts.

This new nozzle design concept provides a way to utilize oxidation and erosion resistant nozzle materials, such as Man Labs' boride alloys, in rocket applications formerly prohibited by thermal shock.

Moderate erosion rates (0.6 mil/sec) of pyrolytic graphite were demonstrated during test firings of a pyrolytic graphite coated Carbitex nozzle. The erosion rates were greater than the 0.075 mils/sec goal of the program.

A washer nozzle containing hafnium pyrocarbide (HfC/PG) and zirconium pyrocarbide (ZrC/PG) washers eroded badly, as did a washer nozzle containing unalloyed pyrolytic graphite. The erosion of the washer nozzles appeared to be caused primarily by mechanical spalling rather than by chemical erosion.

1

Other nozzle concepts, including a ZrC/PG coated Carbitex nozzle and a a HfC/PG coated Carbitex nozzle, were not carried into test firing evaluation because of fabrication difficulties and a program redirection.

It was concluded from this program that the segmented boride nozzle concept has great potential for erosion resistance to N_2O_4/Amine propellants.

SECTION II

SUMMARY

The objective of this program was to develop and demonstrate passively cooled thrust chamber materials capable of withstanding the environment of N_2O_4/Amine propellant combinations for long duration, multiple restart duty cycles. Designs were established with the aid of thermal stress analysis. Test firing evaluation was done at AFRPL at the 3000 lb. thrust level for a chamber pressure of 400 psia exhausting to 13.2 psia. The chamber pressure was to be maintained within five percent over a 300 second firing cycle, which implied an erosion rate of less than 0.10 mil/sec with a throat diameter of about 2.5 inch. It had been estimated that the injector design would produce a maximum wall temperature at the throat of 4000°F.

1. COMBUSTION CHAMBER ENVIRONMENT

a. Temperature

The temperature to which the combustion chamber materials would be exposed would be 3500°F to 4000°F if the engine design goals were met. However, the combustion gas temperatures for the N_2O_4/Amine propellants, some of which are illustrated in Figure 1, are higher than 4000°F for most mixture ratios of interest. Therefore, some form of film cooling or mixture ratio control would be required to limit the chamber material temperatures to 4000°F. This appeared to be feasible with the TRW injector to be used on this program.

b. Chemical Composition

The chemical composition of the combustion gases of interest is typified by that for N_2O_4/MMH shown in Figure 2. The principal corrosive combustion species are H_2O and H_2. Carbon monoxide is inert to the chamber materials of interest, while N_2 will generally be inert or slowly reacting. Carbon dioxide (CO_2) can oxidize many materials, but it is present only in small amounts, especially at low mixture ratios.

A comparison of the H_2O content in the combustion gases of N_2O_4 combined with six amine propellants (MMH, BA 1014, UDMH, N_2H_4 - 0.5 UDMH, and 0.25 NH_3-0.55 N_2H_4 - 0.20 $N_2H_5N_3$) for a range of mixture ratios is shown in Figure 3.

2. MECHANISMS OF OXIDATION PROTECTION

At wall temperatures of 3500°F to 4000°F, the only potential chamber materials which will not be oxidized by the water vapor in the combustion products are oxides. The most refractory oxides are as follows:

3

N$_2$O$_4$ OXIDIZER
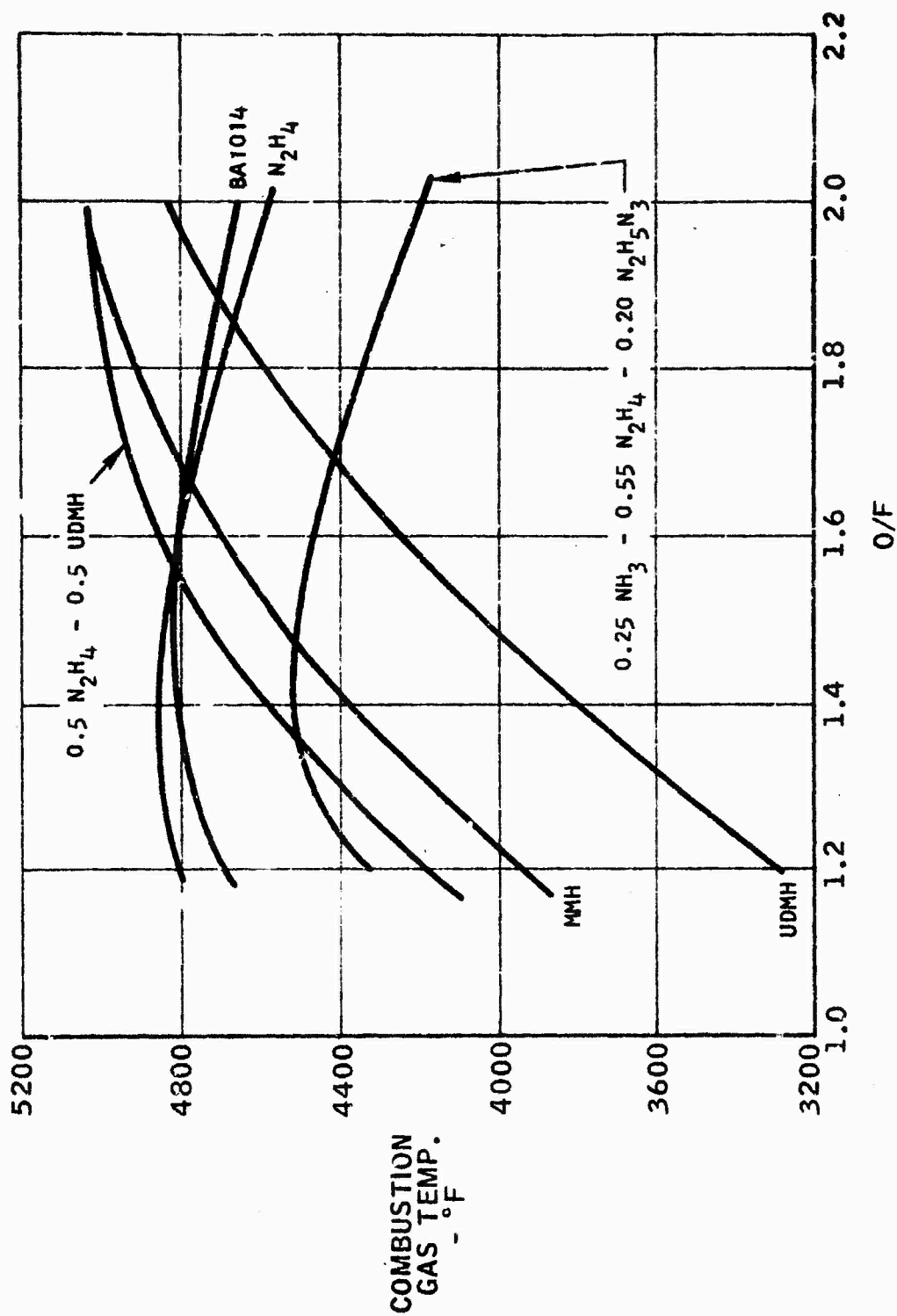
P$_c$ = 400 PSIA   C* EFFICIENCY = 95%

FIGURE 1. ADIABATIC FLAME TEMPERATURE – VS. – O/F

P_c = 400 PSIA η_c^* = 0.95

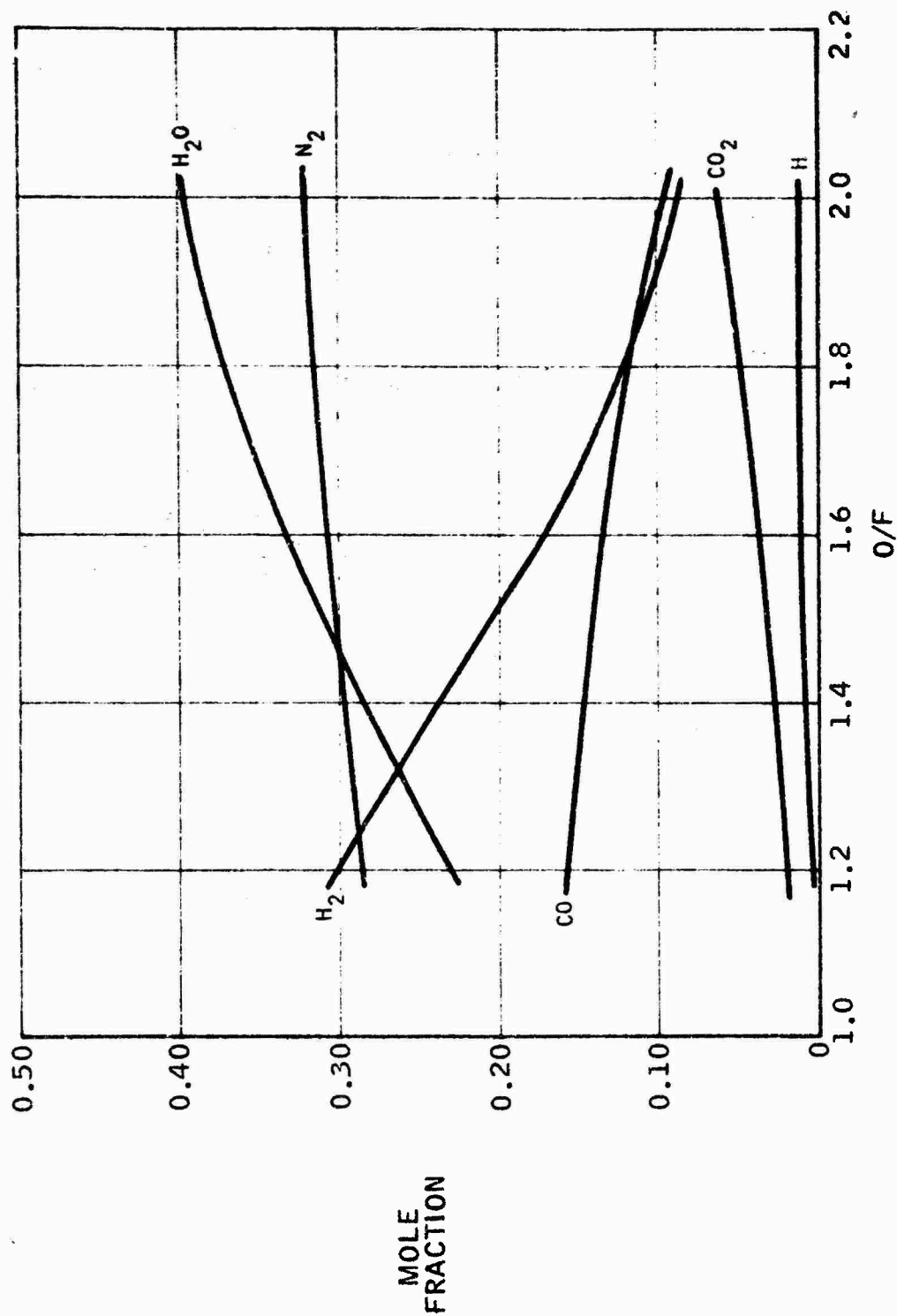FIGURE 2.   COMBUSTION GAS COMPOSITION, N_2O_4/MMH

5
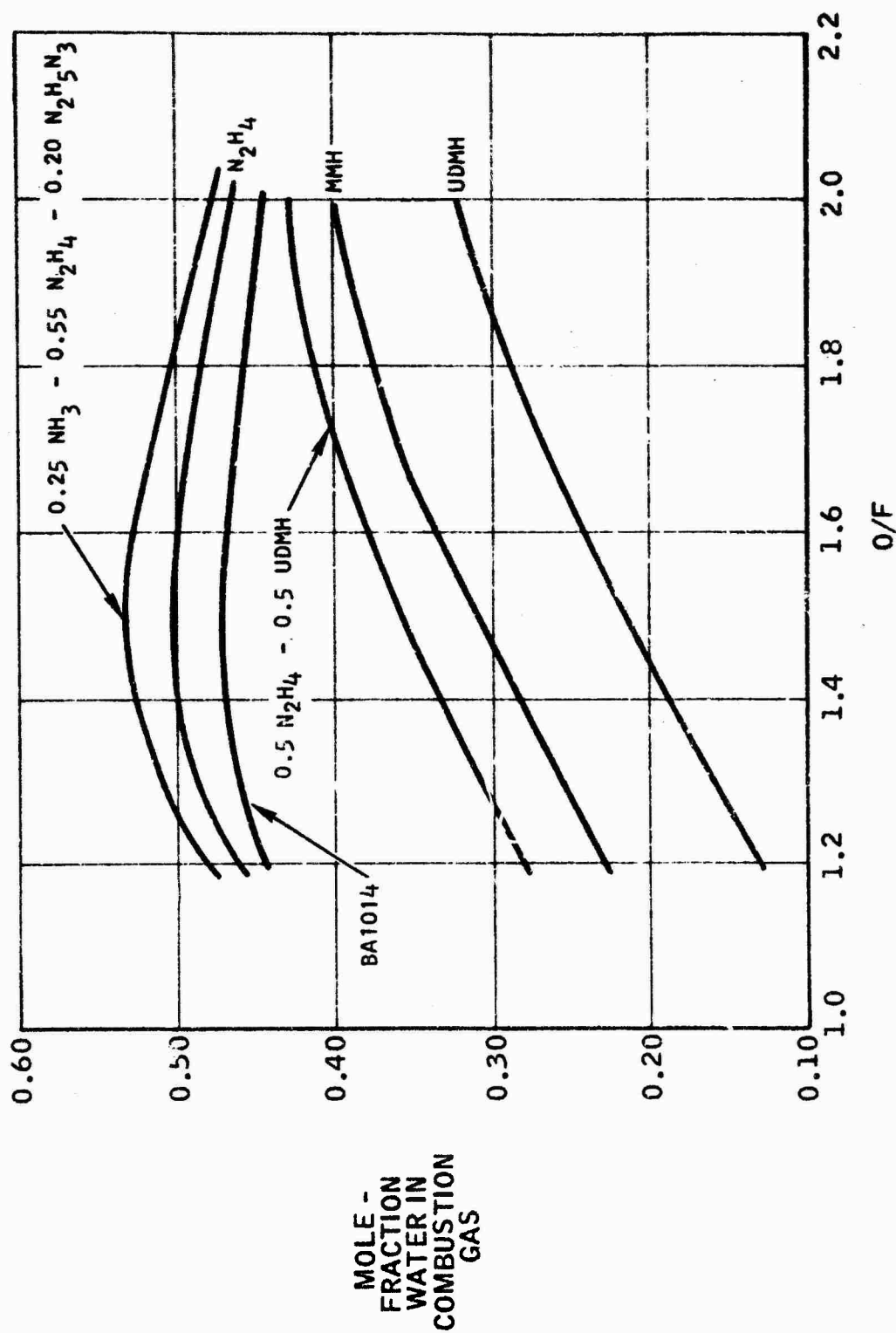
FIGURE 3. COMBUSTION GAS WATER CONTENT, N_2O_4 OXIDIZER

Material	Formula	Melting Point °F
Thorium Oxide	$Th\ O_2$	5970
Hafnium Oxide	$Hf\ O_2$	5252
Magnesium Oxide	MgO	5070
Cerium Oxide	CeO_2	4980
Zirconium Oxide	ZrO_2	4868
Calcium Oxide	CaO	4690
Beryllium Oxide	BeO	4620

Considerable effort has been made to overcome the brittle behavior of the oxides by use of honeycomb metallic reinforcements of various types and by bonding of mixed oxides through sintering, hot pressing, etc. An extensive test firing evaluation of 84 nozzle materials by NASA-Lewis with $N_2O_4/0.5\ N_2H_4$ - 0.5 UDMH at a chamber pressure of 100 psia is reported in Reference 1 . The most successful nozzles tested contained either zirconium oxide or hafnium oxide. Honeycomb reinforced oxides in general have not been very successful in high temperature thermal stress applications.

Another way to use the oxidation resistance of oxidation resistant oxides is to use thrust chamber materials which will form a refractory oxide coating when exposed to the combustion environment. However, in this case the thrust chamber material as well as the resultant oxide must have a melting point above the maximum expected temperature. This limits the number of materials and oxides considerably. Two of the most successful materials which are sufficiently refractory and form refractory oxides are zirconium carbide and hafnium carbide. The melting point of zirconium oxide is 4868°F and that of hafnium oxide is 5252°F. (Variations of several hundred degrees in reported melting points of high temperature materials is common).

Once the oxide surface coating is formed, further oxidation protection depends on the strength of adherence under the combustion gas shearing force, and the rate of diffusion of oxidizing ions through the oxide coating to the virgin material beneath.

Even though an oxide coating is formed on the exposed surface, the wall beneath will be subject to further oxidation. Most of the oxides of interest, such as zirconium and hafnium oxide, are semi-conductors, with metal-deficit lattice structures. However, the number of lattice defects at the oxide-gas interface is expected to be small, and therefore the rate of oxidation through the oxide layer should be somewhat independent of partial pressure of the oxidizing species (Reference 2). This implies that the oxidation rate for a stable oxide coating would not be directly proportional to chamber pressures or gas composition. However, gas shearing force tending to remove the coating will certainly increase with higher chamber pressures. If the oxide does not adhere, the chemical erosion will undoubtedly be excessive for materials such as hafnium carbide and zirconium carbide. The most probable behavior will involve gradually increasing oxide layer thickness, until the strength of the oxide is exceeded, followed by spalling of the oxide layer, with subsequent formation of a new oxide layer. The oxide layer may spall off during cool down and restart, but the amount of total erosion in either case may be acceptable.

7

3. CANDIDATE MATERIALS

The five nozzle materials selected initially for this program were as follows:

a. Zirconium diboride alloy
b. Zirconium pyrocarbide coating on Carbitex
c. Hafnium pyrocarbide coating on Carbitex
d. Zirconium pyrocarbide washers
e. Hafnium pyrocarbide washers.

All of these materials were potentially resistant to oxidation because refractory oxides would form on them when exposed to the combustion gas environment. The zirconium diboride alloys were obtained from Man Labs, Inc. The zirconium pyrocarbide and hafnium pyrocarbide were supplied by the Raytheon Company. The Carbitex was supplied by Carborundum Company.

A sixth nozzle material, pyrolytic graphite coating on PYROBOND, a carbon/carbon composite material, was added soon after the program had begun. It was recognized that the pyrolytic graphite would be subject to chemical erosion. However, it was desired to determine the rate of chemical erosion in a full scale nozzle environment.

The original program plan called for the pyrolytic graphite coating to be applied by Super Temp Company on a carbon/carbon substrate fabricated by Whittaker Corp. and Super Temp Company. The PYROBOND Substrate was not completed, however, due to a program redirection and the pyrolytic graphite coating was evaluated on a Carbitex substrate.

4. PROGRAM REDIRECTION

The program originally called for all six nozzles to be built with a throat diameter of 2.55 inch and tested at 400 psia with N_2O_4/N_2H_4. Considerable difficulty was encountered by Raytheon Company in fabrication of pyrocarbide washers. Concurrently, the Air Force found that one of its rocket programs using a pyrolytic graphite washer nozzle was experiencing excessive erosion. Therefore, a program redirection occurred midway through the program, resulting in emphasis on solving the problems of fabricating pyrocarbide washers for a throat diameter of 1.47 inch. Fabrication of the PYROBOND carbon/carbon composite substrates and the hafnium and zirconium pyrocarbide coated Carbitex nozzles was discontinued, since these materials could not be as easily adapted to the 1.47 inch diameter throat design.

One nozzle was eventually built with both zirconium pyrocarbide and hafnium pyrocarbide washers with a throat diameter of 1.47 inch and tested at a nominal chamber pressure of 570 psia with N_2O_4/MMH. Four other nozzles tested on the program at 400 psia using N_2O_4/N_2H_4 and a throat diameter of 2.55 inch were as follows:

(1 nozzle) ZrB_2, Material V and Material VIII (18, 10)
(1 nozzle) ZrB_2, Material VIII (18, 10)
(2 nozzles)   Pyrolytic graphite coated Carbitex

SECTION III

BORIDE NOZZLE NO. 1

A nozzle assembly with a segmented throat insert of zirconium diboride alloys made by Man Labs, Inc. was designed and fabricated with the configuration shown in Figure 4 . The design was established on the basis of stress analysis of segmented nozzle inserts, which were used in order to allow free thermal expansion and thus reduce the thermal shock stresses below the levels encountered in conventional inserts.

The Man Lab's borides are made from hot-pressed powders of zirconium diboride (ZrB_2) or hafnium diboride (HfB_2) with additives such as silicon carbide (SiC) and/or carbon. When exposed to an oxidizing high temperature environment, the borides oxidize on the surface, forming zirconium oxide (ZrO_2) with a melting point of about $4900^\circ F$, or hafnium oxide (HfO_2), which has a melting point of about $5200^\circ F$. The compositions and observed melting points of a number of Man Labs' borides are shown in Figure 5 . The oxidation resistance has been improved by addition of SiC, which forms a viscous SiO_2 phase, which helps seal the surface and retard further oxidation. Carbon addition to the borides provides a higher thermal conductivity and thermal shock resistance, but reduces oxidation resistance somewhat.

The borides exhibit brittle behavior, being unable to undergo plastic strain at low temperatures. Tests of rocket nozzle inserts have shown that the materials have superior oxidation resistance but fail by cracking. Test firing of small inserts (throat diameter = 0.5 inch) reported in Reference 3 showed that two Man Labs' V inserts incurred axial cracks and/or spalling. Axial cracks indicate probable thermal stress failure due to circumferential thermal stresses exceeding the tensile strength of the material. Spalling failure indicates probable shear failure. The inserts were not designed by thermal stress analysis, but were dimensioned to fit into a standard holder envelope for screening tests. Two other inserts of Man Labs' VIII (18, 10) material were also tested; one had a spall failure and the other had two axial cracks. None of the cracks in Man Labs' materials caused catastrophic failure during testing, probably because of the small size of the inserts. No throat erosion was measured on any of the Man Labs' materials reported in Reference 3 . The tests were run with N_2O_4/Hydrazine at a chamber pressure of about 200 psia and at mixture ratios of 0.73, 1.0 and 1.2, with corresponding combustion temperatures of $4000^\circ F$, $4500^\circ F$ and $5000^\circ F$. The temperatures reached by the inserts during the Reference 3 test durations of up to 120 seconds were not known.

1. STRESS ANALYSIS

Stress analysis of the throat inserts was made using structural networks of the type shown in Figure 6 . Boundary conditions assumed were: (1) outside surface fully restrained and (2) outside surface free to expand. Segment angles (circumferential arc) of 60°, 180° and 360° (continuous axisymmetric ring) were analyzed. Insert thicknesses of 0.1, 0.25, 0.38 and 0.90 inch were evaluated. Transient thermal gradients were calculated assuming a throat film temperature of $4000^\circ F$, based on evaluation of the TRW injector to be used in the test firings.
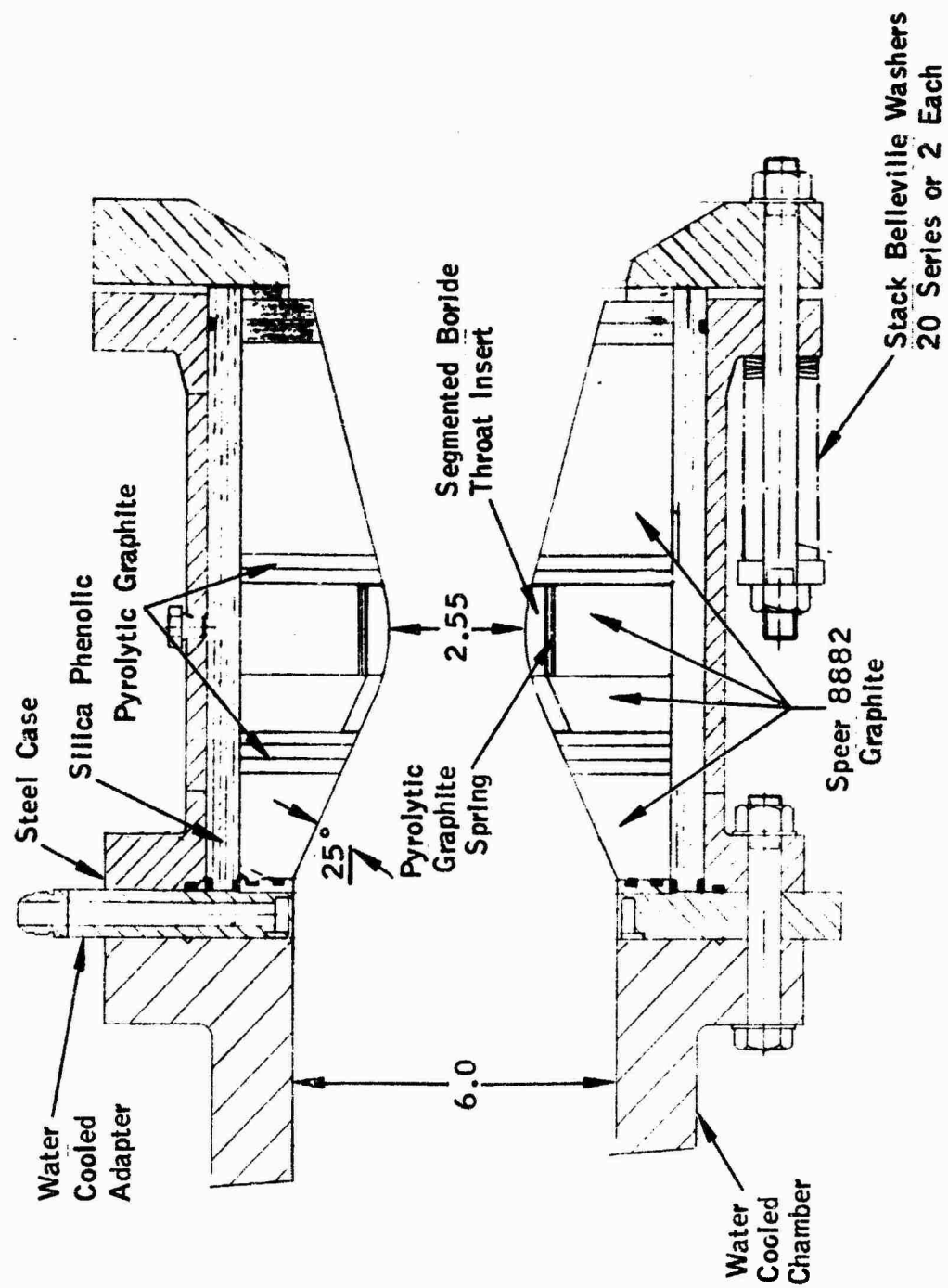
FIGURE 4. DESIGN OF BORIDE NOZZLE NO. 1

Steel Case

Silica Phenolic

Pyrolytic Graphite

Water Cooled Adapter

Pyrolytic Graphite Spring

25°

Segmented Boride Throat Insert

2.55

6.0

Speer 8882 Graphite

Stack Belleville Washers 20 Series or 2 Each

Water Cooled Chamber

10

MELTING POINTS IN INERT ATMOSPHERE

MATERIAL	MELTING POINT °F
HfC	7028
GRAPHITE	6600(S)
ZrC	6386
HfC - GRAPHITE EUTECTIC	5880
HfB_2	5880
ZrB_2	5500
ZrC-GRAPHITE EUTECTIC	5288
SiC	4800
HfO_2	5252
ZrO_2	4868
SiO_2	3100
B_2O_3	650

MELTING POINTS OBSERVED IN AIR ARC PLASMA

DIBORIDE MATERIAL	COMPOSITION (VOLUME %)	LIQUID OXIDE °F	LIQUID DIBORIDE °F
I	ZrB_2	4690	5580
II	HfB_2	5250	6200
III	HfB_2, SiC (20)	4800	5620
IV	HfB_2, SiC (30)	5070	5410
V	ZrB_2, SiC (20)	4480	5390
VIII (18,10)	ZrB_2, SiC (18), C (10)		
VIII (14,30)	ZrB_2, SiC (14), C (30)	4830	4980
XIV (18,10)	HfB_2, SiC (18), C (10)		
XIV (14,30)	HfB_2, SiC (14), C (30)		

FIGURE 5. MELTING POINTS OF OXIDATION RESISTANT MATERIALS

11

FIGURE 6. STRUCTURAL NETWORK FOR BORIDE NOZZLE STRESS ANALYSIS

12

The temperature gradients in a 3/8-inch thick insert are shown in Figure 7 .
Material properties of Material V (80% ZrB_2, 20% SiC) shown in Table I , were
used for almost all of the stress analysis. Preliminary analysis of maximum stresses
due to linear temperature gradients were made using the following equation from
Reference 4 :

$$\sigma_\theta = \sigma_z = \frac{\alpha E \Delta T}{2(1-\nu) \ln \frac{b}{a}} \left(1 - \frac{2a^2}{b^2 - a^2} \ln \frac{b}{a}\right)$$

Where:

σ_θ = Circumferential stress, outside surface

σ_z = Axial stress, outside surface

α = Coefficient of thermal expansion

E = Modulus of elasticity

ΔT = Linear temperature gradient

ν = Poisson's ratio

a = Inside radius of insert

b = Outside radius of insert

The predicted stresses for Material V and Material VIII (18, 10) differed by only
12% for equal temperature gradients, as might be expected from examination of material
properties in Table I . Therefore, subsequent stress predictions for Material V, using
temperature dependent material properties and transient temperature gradients, were
also assumed to be applicable to Material VIII (18, 10). These two materials were selected
from the large number of Man Labs' boride alloys, Figure 5 , because Man Labs has
had more experience in fabricating and testing these two than any others. It was expected
that they would also be somewhat more oxidation resistant than Material VIII (14, 30),
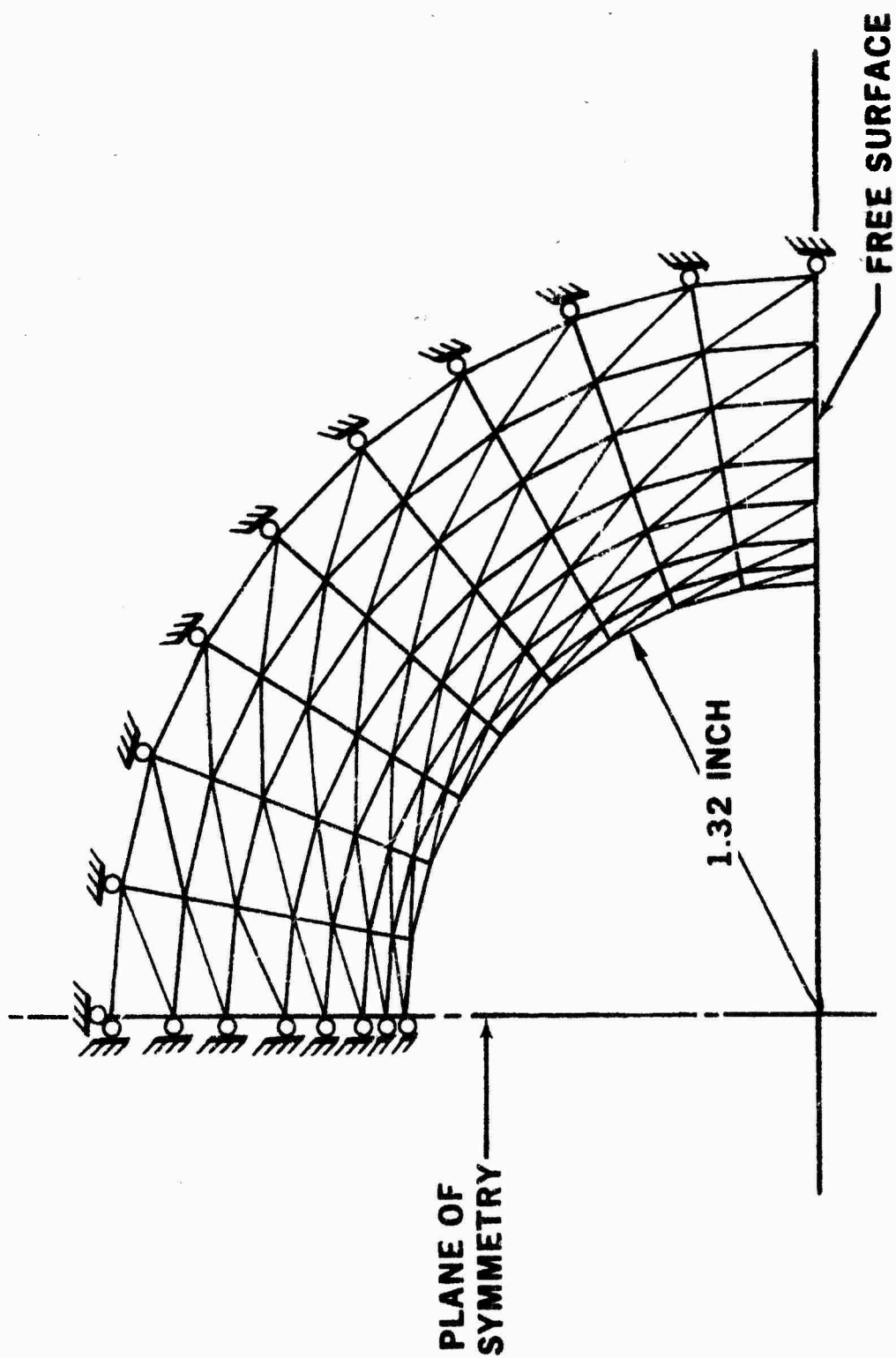which contains a larger amount of carbon to allow easy machining.

Since the borides are brittle materials, maximum principal stress exceeding tensile
strength was assumed to be the failure criterion. The effects of various types of inserts
and external boundary conditions are shown in Figure 8 . These results, for a throat
insert thickness of 0.96-inch, should be representative of boundary condition effects for
other thickness inserts. It is shown in Figure 9 that a continuous ring insert (360°
segment) reaches a maximum principal stress early in the firing, and then experiences
reduced stresses as the insert temperature approaches steady state. If the insert is
split into two 180° segments, and is free to expand radially, the maximum principal stress
is reached much earlier in the firing, and is only about half of the magnitude of stress
reached in continuous ring inserts. The thermally expanded shape of such an insert is
shown in Figure 10 .
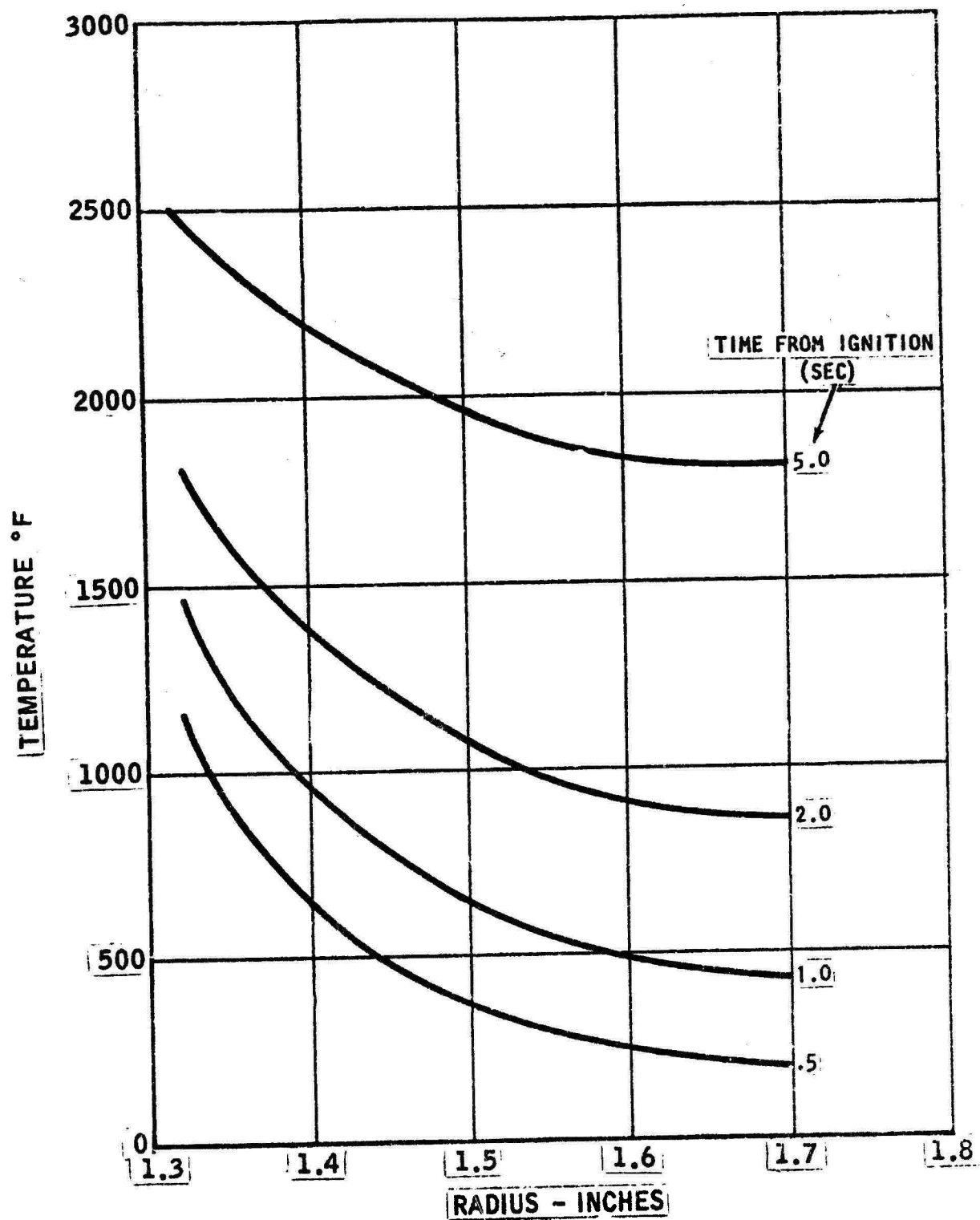
FIGURE 7. TEMPERATURE DISTRIBUTION IN 3/8 IN. BORIDE INSERT

14
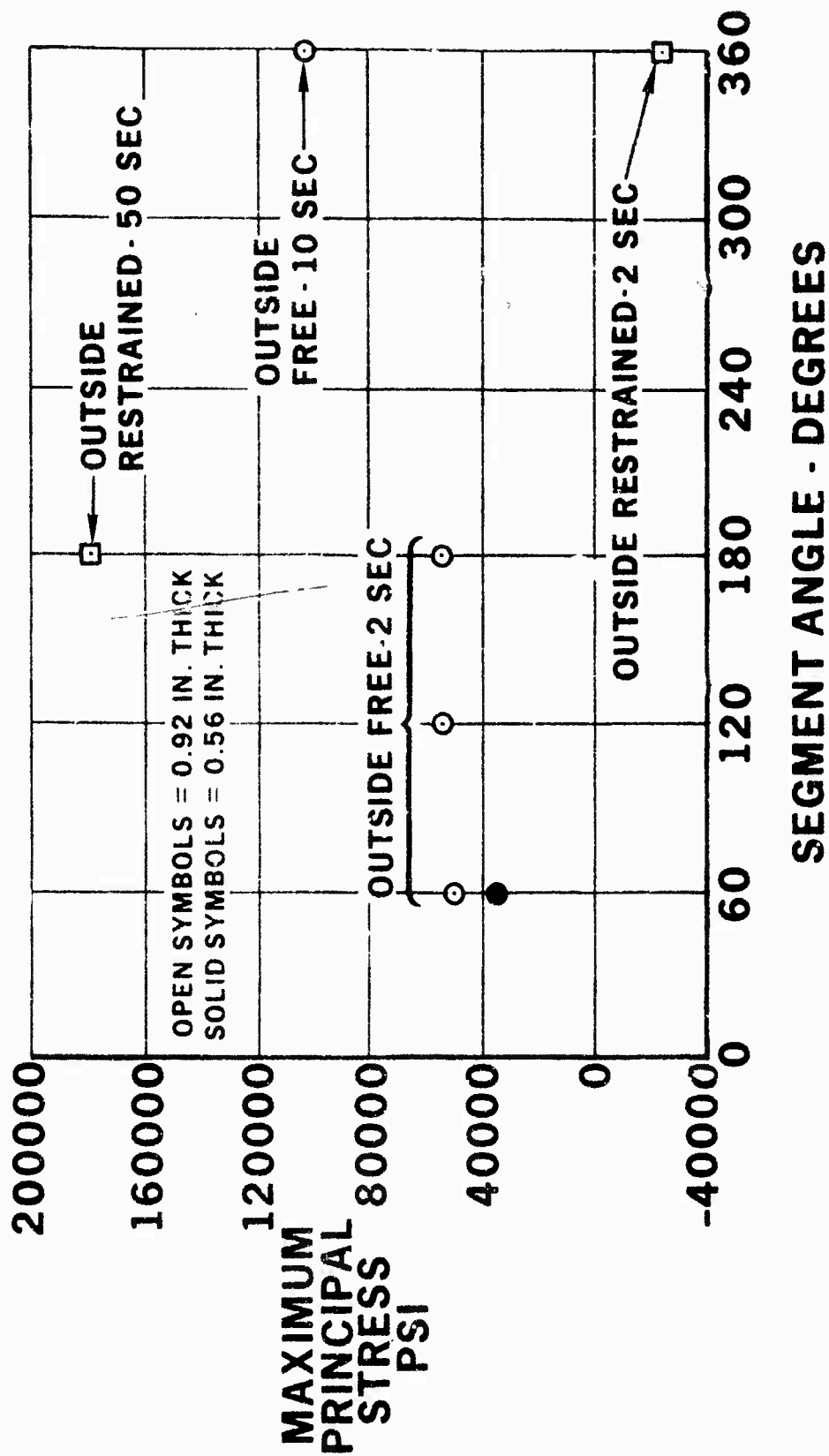
FIGURE 8. MAXIMUM STRESS FOR VARIOUS INSERT CONFIGURATIONS
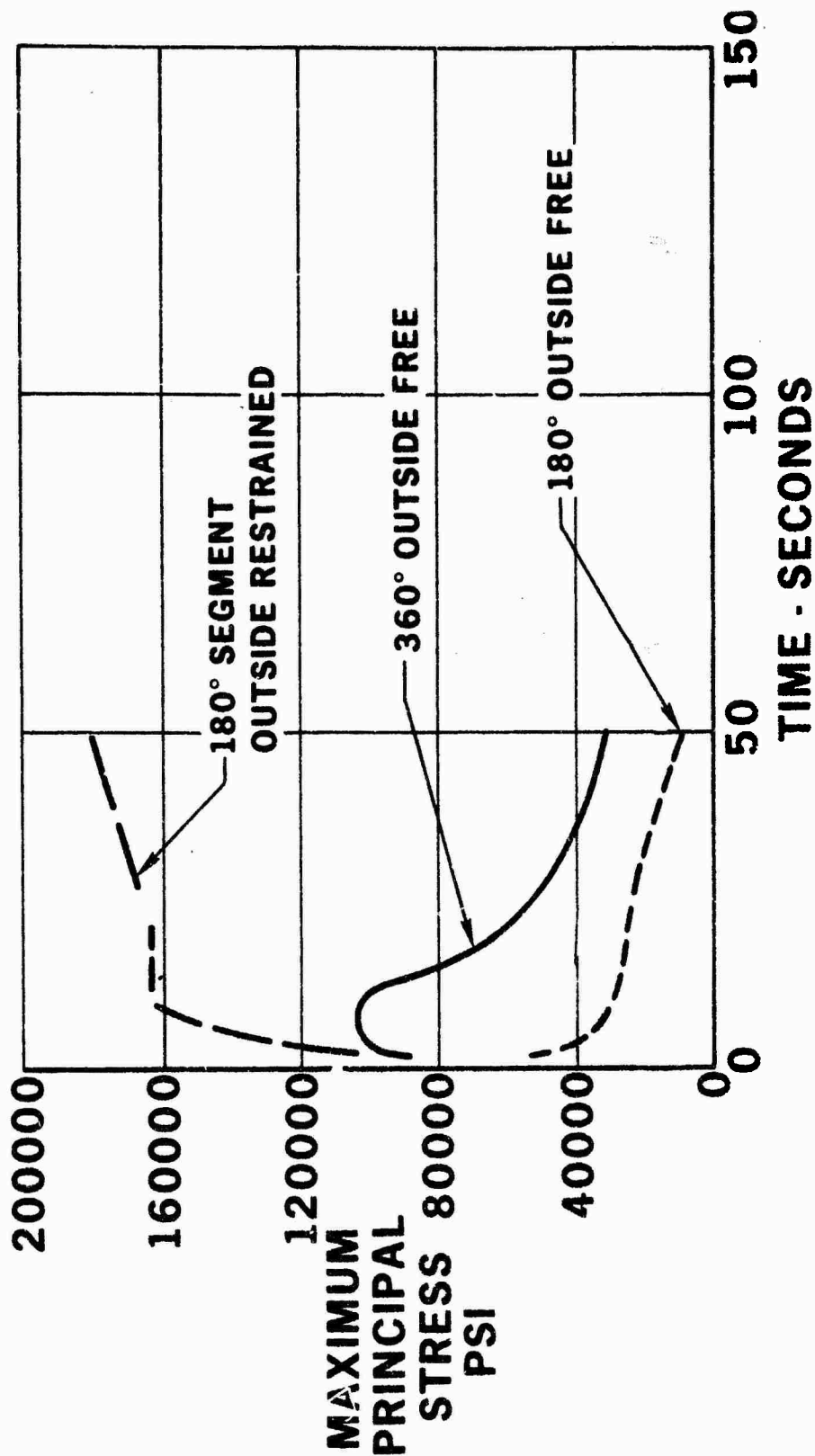
FIGURE 9. STRESS-VS-TIME, PLANE STRESS CONDITION

16
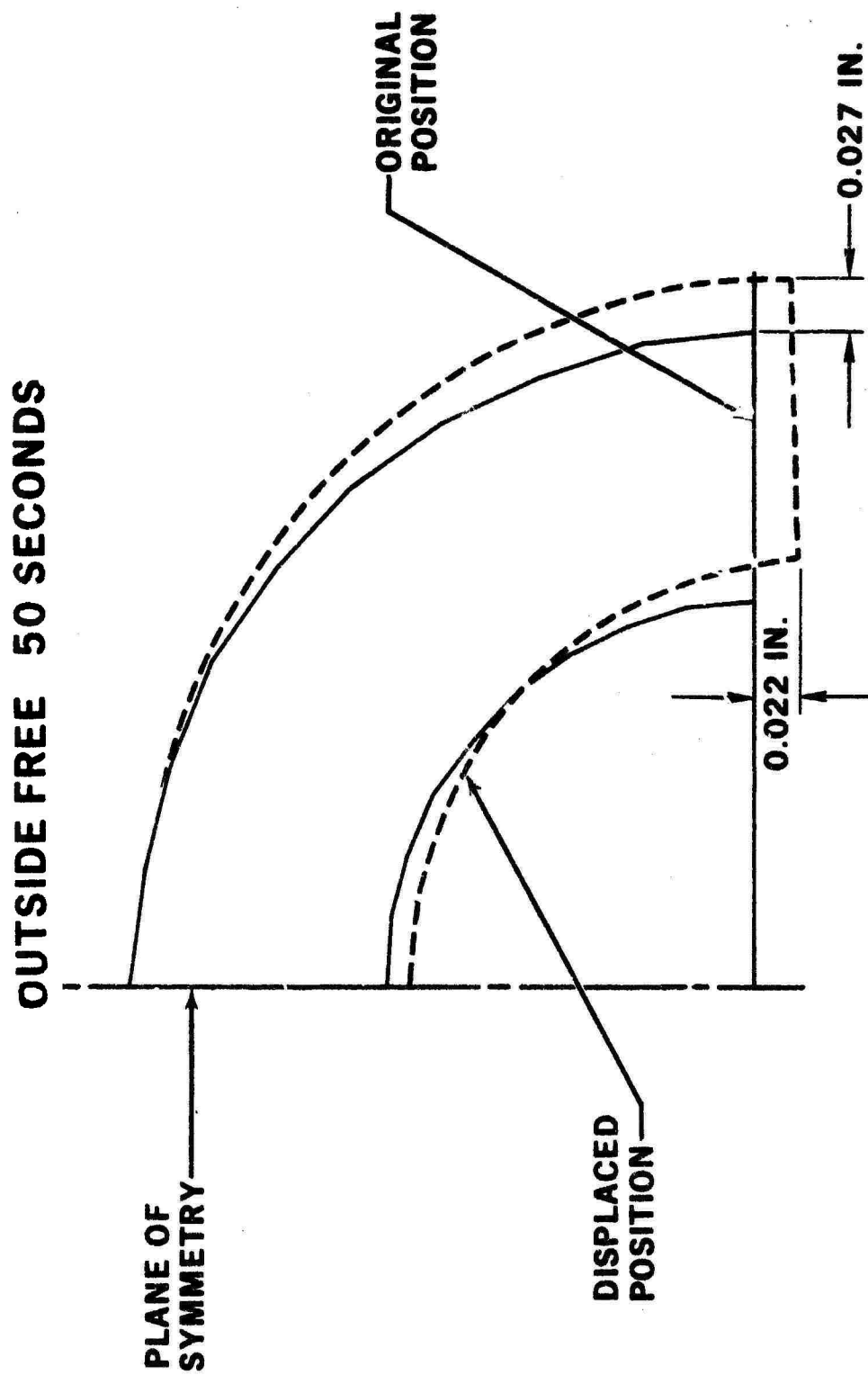
FIGURE 10. DEFLECTED CONTOUR, 180 DEGREE SEGMENT

TABLE I

ENGINEERING PROPERTY DATA FOR MAN LABS' ZIRCONIUM DIBORIDE COMPOSITIONS V, VIII (18, 10), AND VIII (14, 30)

Temp. °F	Bend [1][2] Strength 10³ lbs/in²			Elastic Modulus 10⁶ lbs/in²			Coefficient of Thermal Expansion in/in-°F		
	MATERIAL V	MATERIAL VIII 18,10	MATERIAL VIII 14,30	MATERIAL V	MATERIAL VIII 18,10	MATERIAL VIII 14,30	MATERIAL V	MATERIAL VIII 18,10	MATERIAL VIII 14,30
80	48	52	41	76	68	30	3.3 (From 80 to 3300° F)	3.9	3.6
620	49	62	42	74	68	30			
1160	51	60	43	72	66	30			
1700	47	50	44	70	66	30			
2240	38	40	45	67	60	30			
2780	32	38	46	64	60	30			
3320	32	36	47	–	–	–			

Temp. °F	Density lbs/ft³			Heat Capacity BTU/lb°F			Thermal Conductivity BTU/ft·hr·°F		
	MATERIAL V	MATERIAL VIII 18,10	MATERIAL VIII 14,30	MATERIAL V	MATERIAL VIII 18,10	MATERIAL VIII 14,30	MATERIAL V	MATERIAL VIII 18,10	MATERIAL VIII 14,30
80	342	331	280	0.100	0.102	0.108	60	61	45
620	340	329	279	0.150	0.158	0.178	51	55	42
1160	337	327	277	0.160	0.175	0.195	48	47	37
1700	335	325	276	0.170	0.180	0.216	46	44	34
2240	333	323	274	0.176	0.185	0.227	44	40	32
2780	331	321	273	0.184	0.193	0.238	42	38	30
3320	329	319	272	0.189	0.200	0.247	40	36	28
3600	327	317	270	0.193	0.205	0.256	39	35	27

(1) Bend Strength Values Obtained from 4-point Loaded Beam Test.

(2) Material V Room Temperature Compressive Strength: 500,000 lbs/in².

18

If the segmented insert is not allowed to expand radially, the maximum principal stress continues to rise with firing time, as shown in Figure 10 . Therefore, it is important that room for expansion be provided around a segmented insert.

The effect of segment arc angle is shown in Figure 8 for a condition of plane stress. It is shown that the first split in the insert is the most effective, with stresses of about 100,000 psi in a continuous 360° insert dropping to about 50,000 psi for a 180° segment. Additional reduction in arc angles to 60° does not cause much greater reduction in stress. Therefore, the final stress analyses to select the best insert thickness were made for 180° throat segments.

A summary of the predicted stresses for various insert thicknesses is shown in Table II . An insert length of 1.6 inches was used in all of these calculations. Other analyses have shown that axial stresses could be reduced by using shorter inserts, but maintenance of throat contour over as great a length as possible was also desirable.

2. INSERT DESIGN

It is shown in Table II that stresses are higher for plane strain rather than plane stress conditions, and that maximum stress increases with insert thickness. The predicted stresses were compared with room temperature strength of the borides, since the peak of stresses occurred at locations and firing durations for which the temperature had not yet increased significantly. It was desirable to use as thick an insert as possible because it would help retention by the aft pyrolytic graphite washer. The magnitude of pyrolytic graphite erosion was not know, but was predicted theoretically to be negligible for the first 50 seconds, rising to about 0.050 inch after 150 seconds. More important, the amount of throat erosion was unknown, and a thicker insert could better stand some fair amount of erosion. Consideration of such factors led to the choice of a 0.38-inch thick insert (O. D. of 3.30 inches, throat diameter of 2.55 inches).

The use of a segmented throat insert offered the opportunity to use two different boride alloys in one nozzle assembly. Material V was chosen as one material because it does not contain carbon and would, therefore, be expected to have maximum oxidation resistance. Material VIII (18, 10) was chosen as the second material, since it has the characteristic of unusually high tensile strength in the direction perpendicular to the pressing direction, as shown in Figure 11 . The pressing direction would ordinarily be along the billet (and engine) axis, so that the high strength would be in the circumferential direction. The anisotropy of tensile strength of Material VIII (18, 10) is due to the orientation of graphite particles during pressing.

It was recognized that strength of the throat inserts was marginal, but the design represented a compromise between predicted stresses, strength, and unknown erosion of the insert and backup pyrolytic graphite washer.

A continuous ring of Material V was located just upstream of the throat segments. No stress analysis was done on the upstream ring, but it was expected to crack from thermal stresses, based on the stress analysis of the throat inserts. It was hoped, however, that the cracked upstream segment would remain in place, providing a smooth flow contraction and minimizing erosive forces on the throat segments.

19
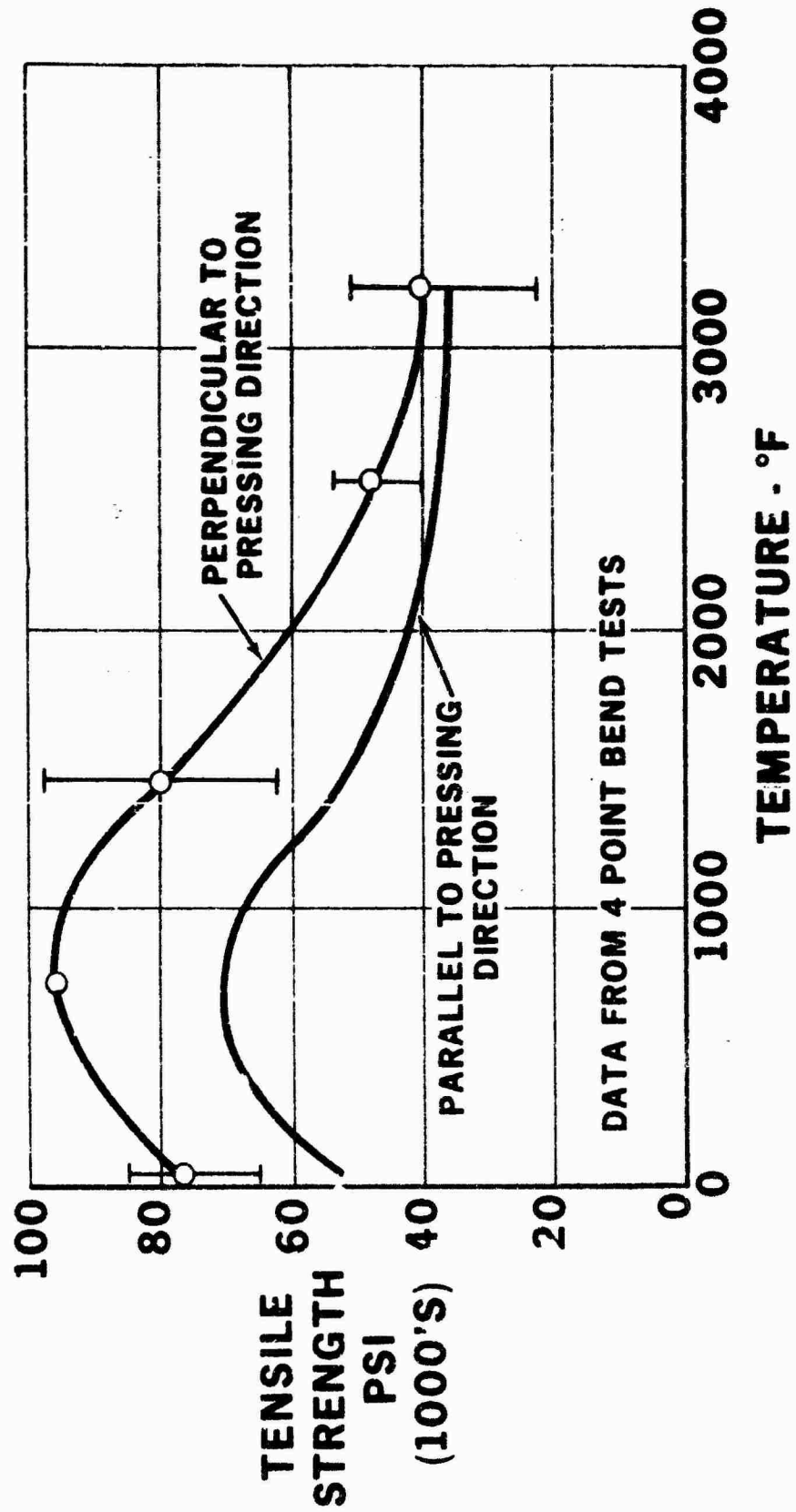
FIGURE 11. ANISOTROPY OF STRENGTH, MATERIAL VIII (18, 10)

20

TABLE II

SUMMARY OF STRESS ANALYSIS

MANLABS MATERIAL V

| | Unrestrained Ring | | | | | | | 180° Segment | | | | |
| | t = .1" | | t = .25" | | t = .38" | | t = .96" | t = .25" | | t = .38" | | t = .96" |
τ Sec.	σ_z	σ_θ	σ_z	σ_θ	σ_z	σ_θ	Principal Plane Stress	Principal Stress Plane Stress	Principal Stress Plane Strain	Principal Stress Plane Stress	Principal Stress Plane Strain	Principal Stress Plane Stress
.05	44,637	47,597										
.1	49,109	52,117	61,700	65,921								
.2												
.3	45,808	48,778	73,992	78,641					49,953			
.4												
.5	39,598	42,499	73,825	78,416	80,580	90,809		32,705	48,456	41,240	54,951	
1.	28,296	31,079	66,924	71,129	85,668	96,451	–		43,800		56,800	
1.5			57,818	61,573	83,033	93,539	–		42,958		56,194	
2			50,150	53,537	79,400	89,438	–				50,627	53,000
4							–					
150							–					

21

Detailed design of the boride inserts is shown in Figure 12. A pyrolytic graphite leaf spring was placed in the gap outside of the throat segments to keep the segments centered in the throat during ignition and firmly constrained during handling and vibration.

The boride inserts were fabricated by Man Labs, Inc., Cambridge, Mass. The assembly of the two throat inserts and the pyrolytic graphite springs is shown in Figure 13.

3.   TEST FIRING EVALUATION

The No. 1 Boride Nozzle Assembly shown in Figure 4 , was test fired at AFRPL using N_2O_4/N_2H_4 propellants, at a mixture ratio of 1.15. The C* efficiency was 78.5%. The nozzle failed and the firing was terminated after 47.6 seconds. The first significant drop in chamber pressure, from about 380 psig to 350 psig, occurred 12 seconds after ignition. The chamber pressure had risen slightly by about 10 psi just before the sudden drop in pressure at 12 seconds. The chamber pressure dropped gradually from 350 psig to about 338 psig at 30 seconds after ignition, at which time a sudden drop in chamber pressure to 315 psig occurred, followed by gradual decline to 285 psig at the time of shutdown.

Post test examination of the nozzle showed that all three segments of boride had been ejected from the nozzle. Small fragments of boride shown in Figure 14 were picked up near the test site. The thickness or shape of most of the fragments was sufficiently clear to distinguish between the upstream insert and the throat segmented inserts. Photomicrographs of some of the throat fragments were taken, which provided identification of the material composition (either Material V or Material VIII (18, 10). The results of the visual and microstructural evaluation are summarized in Table III The amount of oxide on the Material VIII (18, 10) fragments was much greater than that on the Material V fragments from either the upstream ring or the throat segment.

The following conclusions were drawn from the post test evaluation of Boride Nozzle No. 1:

a.   The upstream ring of Material V cracked into small pieces and was ejected immediately after ignition. It was expected that the upstream ring would suffer thermal stress cracking, based on approximate comparisons with the extensive stress analysis done on throat ring inserts and segmented throat inserts. However, it had been hoped that the upstream ring would remain in place. The crack propagation was evidently so severe that the upstream ring broke into fragments small enough to pass through the throat.

b.   The throat segment made of Material V cracked and was ejected from the nozzle immediately after ignition. The maximum thermal stress in the throat insert had been calculated to be 56,800 psi one second after ignition, assuming instantaneous chamber pressure of 400 psia. The

22
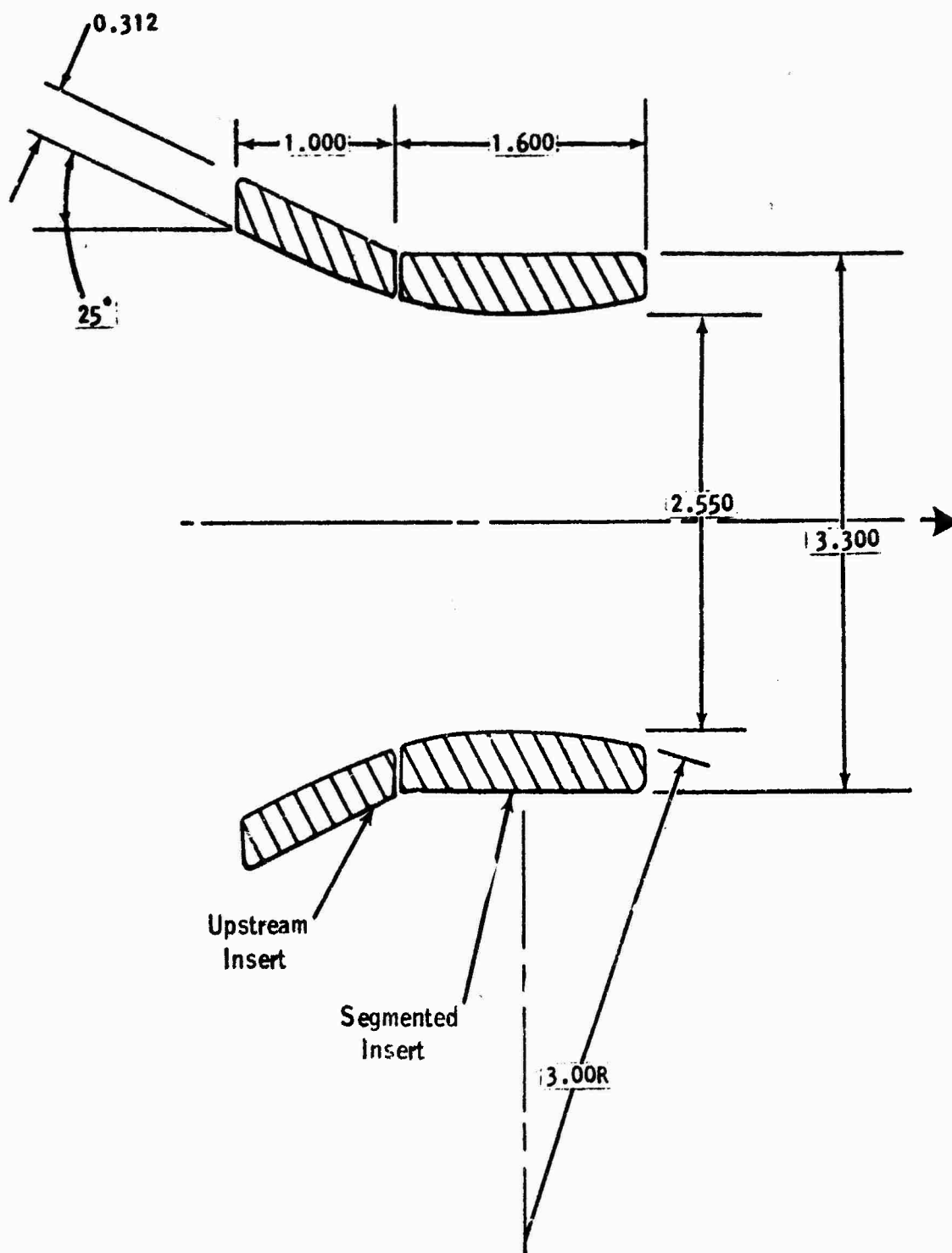
FIGURE 12. DESIGN OF INSERTS FOR BORIDE NOZZLE NO. 1

23

FIGURE 13. INSERT ASSEMBLY, BORIDE NOZZLE NO.1

FIGURE 14. FRAGMENTS OF SEGMENTED NOZZLE

TABLE III

POST TEST EXAMINATION OF BORIDE FRAGMENTS

Specimens Collected After Test Firing June 7, 1972

Specimen	Material Identification	Visual Appearance
Throat Specimen No. 1	Material V	No significant oxidation
Throat Specimen No. 2	Material V	Some slight oxidation
Throat Specimen No. 3	Not Analyzed	Some slight oxidation
Throat Specimen No. 4	Material VIII (18, 10)	Covered with white oxide and sand from ground
Upstream Specimens No's. 1, 2, 3	Material V	No significant oxidation
Unidentified Specimens	-	Heavy white oxide coating

actual chamber pressure rise took about 0.4 second, but this reduction of the thermal stress environment was not sufficient to avoid thermal stress failure. The strength of Material V is only 48,000 psi, and it had been recognized that the design was marginal in strength.

c.   The throat segment made of Material VIII(18, 10) was not ejected from the nozzle until 30 seconds after ignition. The sequence of events cannot be established with certainty, but the best explanation is that after ejection of the Material V throat segment, the Material VIII (18, 10) segment was free to move transversely a distance of about 0.5-inch, which would allow gas flow around the insert and would produce bending moments in the axial and possibly radial directions. Evidently this condition prevailed until the insert reached a temperature at which its tensile strength was exceeded by the bending stresses. There is no strength data available for the borides above 3300°F, and the insert probably reached 4000°F or higher. The room temperature strength of Material VIII (18, 10) is anisotropic, being about the same as Material V in the pressing (axial) direction, but being significantly higher (75,000 psi) in the circumferential direction, perpendicular to the pressing direction. It was concluded that the strength of the Material VIII (18, 10) was sufficient to withstand the thermal stress just after ignition, whereas Material V failed.

SECTION IV

BORIDE NOZZLE NO. 2

1. DESIGN

A second boride nozzle, shown in Figure 15, was designed after post test evaluation of the first boride nozzle. Both 160°F throat segments were made of Material VIII (18, 10). The upstream boride ring was eliminated and replaced by pyrolytic graphite washers. The length of the throat inserts was reduced to approximately 0.60-inch in order to reduce axial stresses. The throat inserts were also made thicker (0.52-inch) than in boride nozzle No. 1, with an outside diameter of 3.60 inches instead of 3.30 inches. The design of the throat segments for boride nozzle No. 2 is shown in Figure 16. Pyrolytic graphite springs were used as in boride nozzle No. 1. Radial slots were milled on the face of the downstream pyrolytic graphite washer which retained the throat segments. The slots were designed to maintain pressures surrounding the throat segments which would be lower than the average pressure on the inside of the inserts. This should eliminate the possibility of ejecting the insert in case of cracking.

An oxide coating was provided on the inside surface by pre-oxidation and subsequent grinding of all surfaces except the inside surface and ends. The pre-oxidized throat segments are shown in Figure 17. It was calculated that an oxide layer of 0.006-inch would reduce the heat flux into the insert by about 50% if it would adhere during the early stages of engine firing.

The coating formed by preoxidation was not uniform in appearance, as shown in Figure 17. The coating was a mixture of glassy SiO_2 and white ZrO_2. A pyrolytic graphite ring of the size desired to fabricate the pyrolytic graphite springs could not be procured due to lack of funds at this point of the program. Therefore, an available pyrolytic graphite ring was used to make the four springs. After cutting the springs, their stiffness was found to be much greater than desired, but assembly of the Segmented Nozzle No. 2 with these springs was possible.

The incorporation of the design changes described above, together with the relatively good performance of the Material VIII (18, 10) insert, indicated a good probability of accomplishing a successful firing with Boride Nozzle No. 2.

2. TEST FIRING EVALUATION

Boride Nozzle No. 2 was test fired successfully with excellent results. A first firing of 25 seconds was made with the propellant combination $N_2/O_4/N_2H_4$ at a mixture ratio of 0.94. The C* efficiency was 94.5%. The chamber pressure was 401 psig during the 25-second firing, after which the nozzle was removed from the stand, examined, and photographed. The nozzle entrance after the 25-second firing

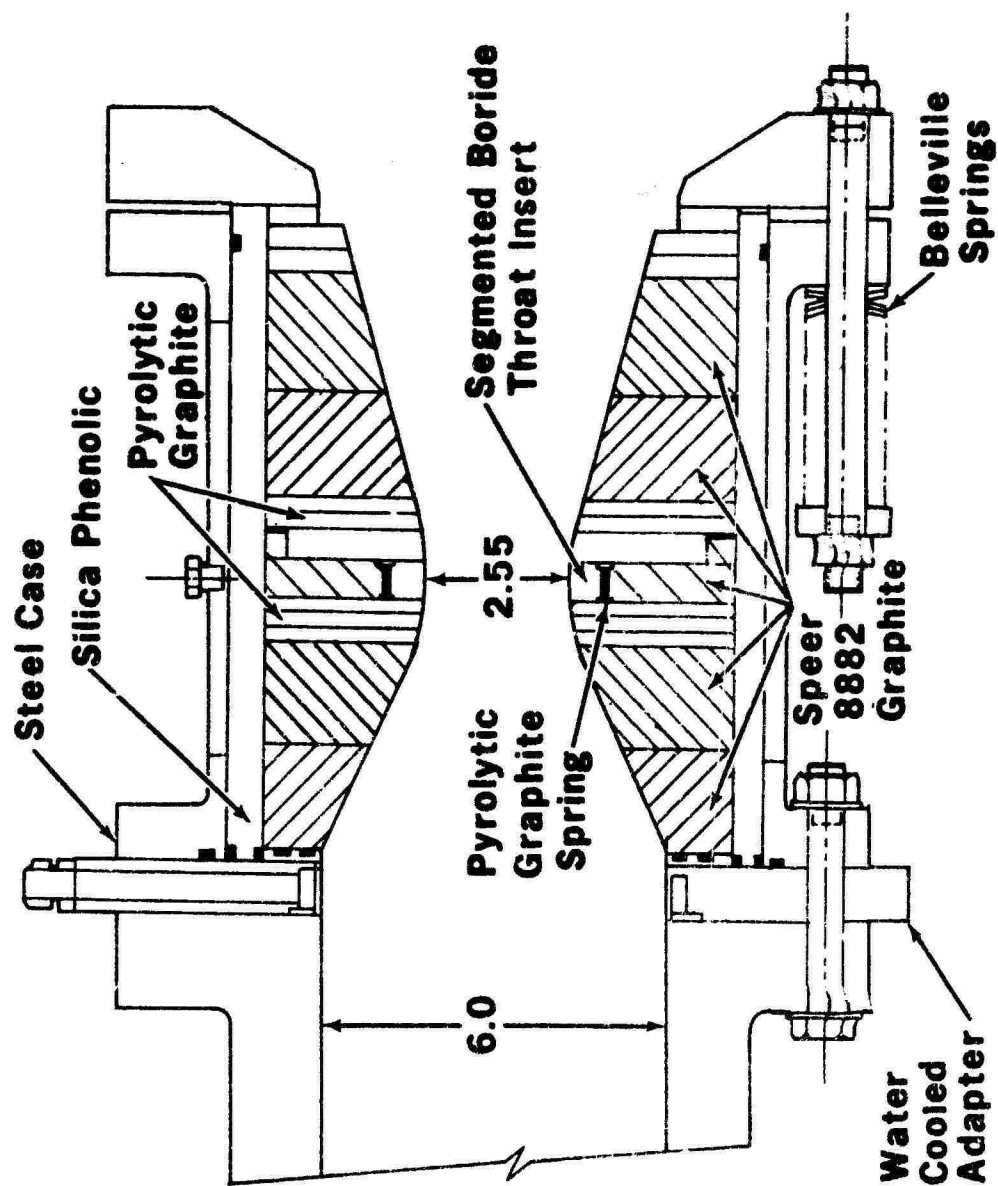# SEGMENTED PRE-OXIDIZED BORIDE NOZZLE
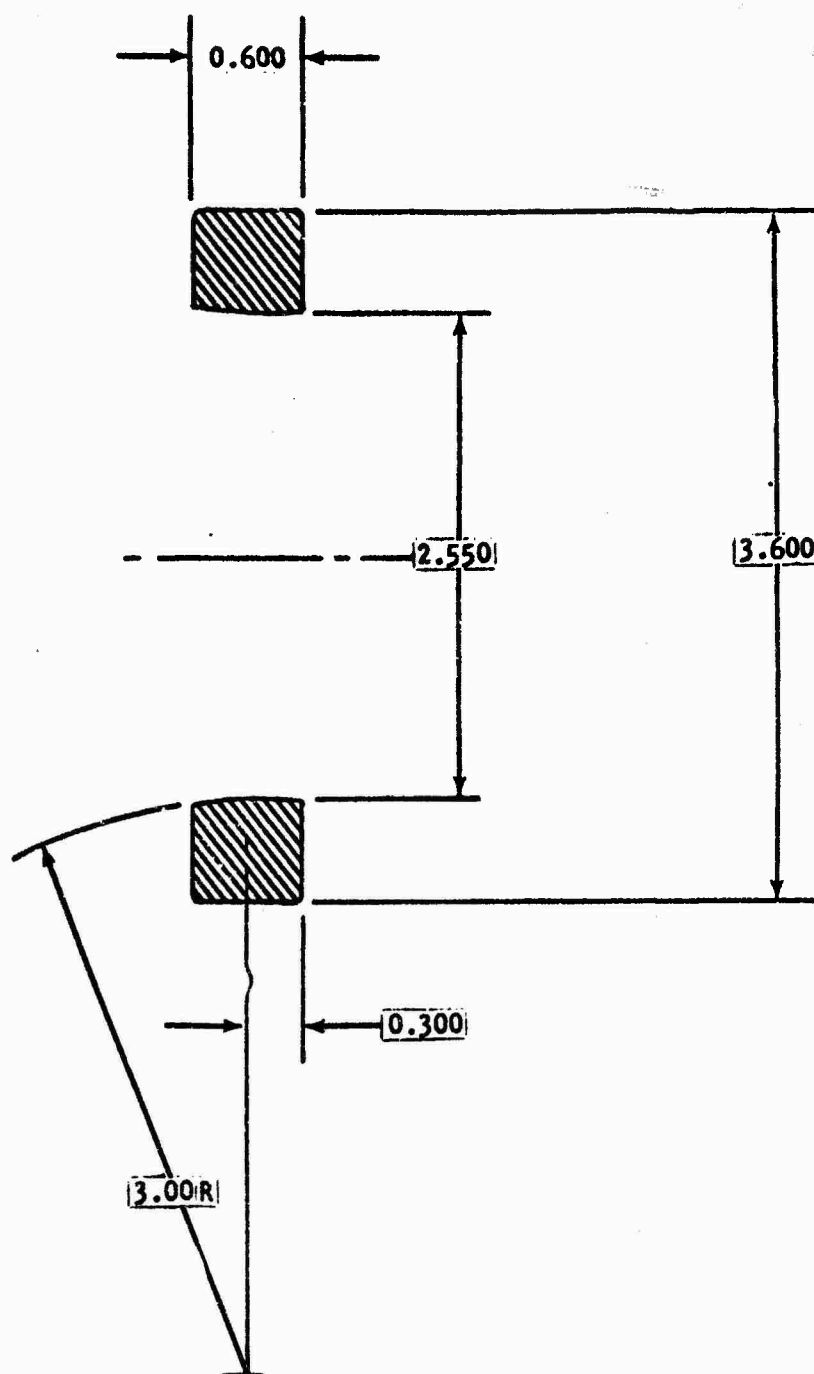

FIGURE 15. DESIGN OF BORIDE NOZZLE NO. 2

29

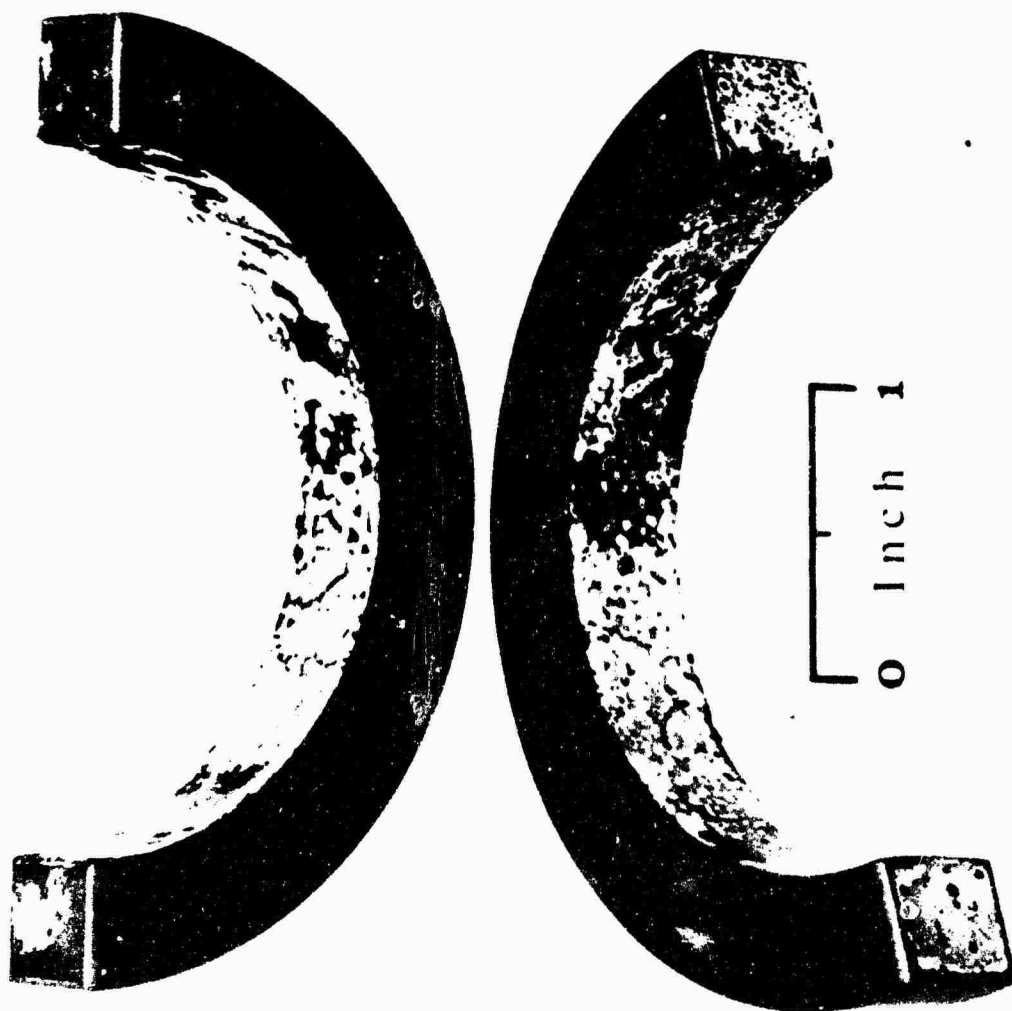FIGURE 16. THROAT INSERT FOR BORIDE NOZZLE NO. 2

FIGURE 17. PREOXIDIZED THROAT SEGMENTS

0 Inch 1

is shown in Figure 18. There was no measurable throat erosion and the oxide layer on the boride segments seemed to be in the same condition as before the firing. It seemed probable that the pre-oxidized coating had adhered throughout the engine firing. There were no visible cracks in the boride segments.

The first test firing had been terminated at 25 seconds because of a mechanical failure of the injector pintle, causing a large drop in performance and chamber pressure. After replacement of the pintle, a second firing was made for 53 seconds at a mixture ratio of 0.93. The C* efficiency was 84.5%. The firing was terminated because of overheating of the injector, causing an excessive rise of fuel manifold pressure. A very slight drop in chamber pressure was noted during the 53-second firing, from 360 psig to 357 psig. The nozzle throat is shown in Figure 19. There was evidence of some slight erosion, and several cracks in the boride segments. The boride segments and pyrolytic graphite springs are shown after disassembly of the nozzle in Figure 20.

The cracks in the boride segments were apparently caused by cracking and displacement of one of the pyrolytic graphite springs, which prevented full thermal expansion of the segments as they approached steady state temperature. This condition is described by the results of stress analysis of 180 degree segments, restrained on the outside surface, as shown in Figures 8 and 9. The fact that the PG springs were overstressed is also indicated by the delamination seen in one spring.

The effects of the bypass flow of gas around the boride segments and through the slots in the aft PG washer are shown by the oxidation streaks on the aft side of the boride segments, as shown in Figure 21. This bypass gas flow did not seem to cause any problem in the nozzle insert.

The results of the post test evaluation of Boride Nozzle No. 2 lead to the following conclusions:

a.   The thermal stresses in the pre-oxidized segmented nozzle did not cause any cracking of the boride at the time of peak thermal stress just after ignition or during the 25 second firing.

b.   The available pyrolytic graphite springs cracked and displaced during the 53 second firing due to excessive stiffness, leading to stress failure as the insert approached steady state temperatures.

c.   Use of a proper pyrolytic graphite spring or other design changes to prevent displacement of the pyrolytic graphite springs should permit use of segmented nozzle inserts for a variety of firing duty cycles.

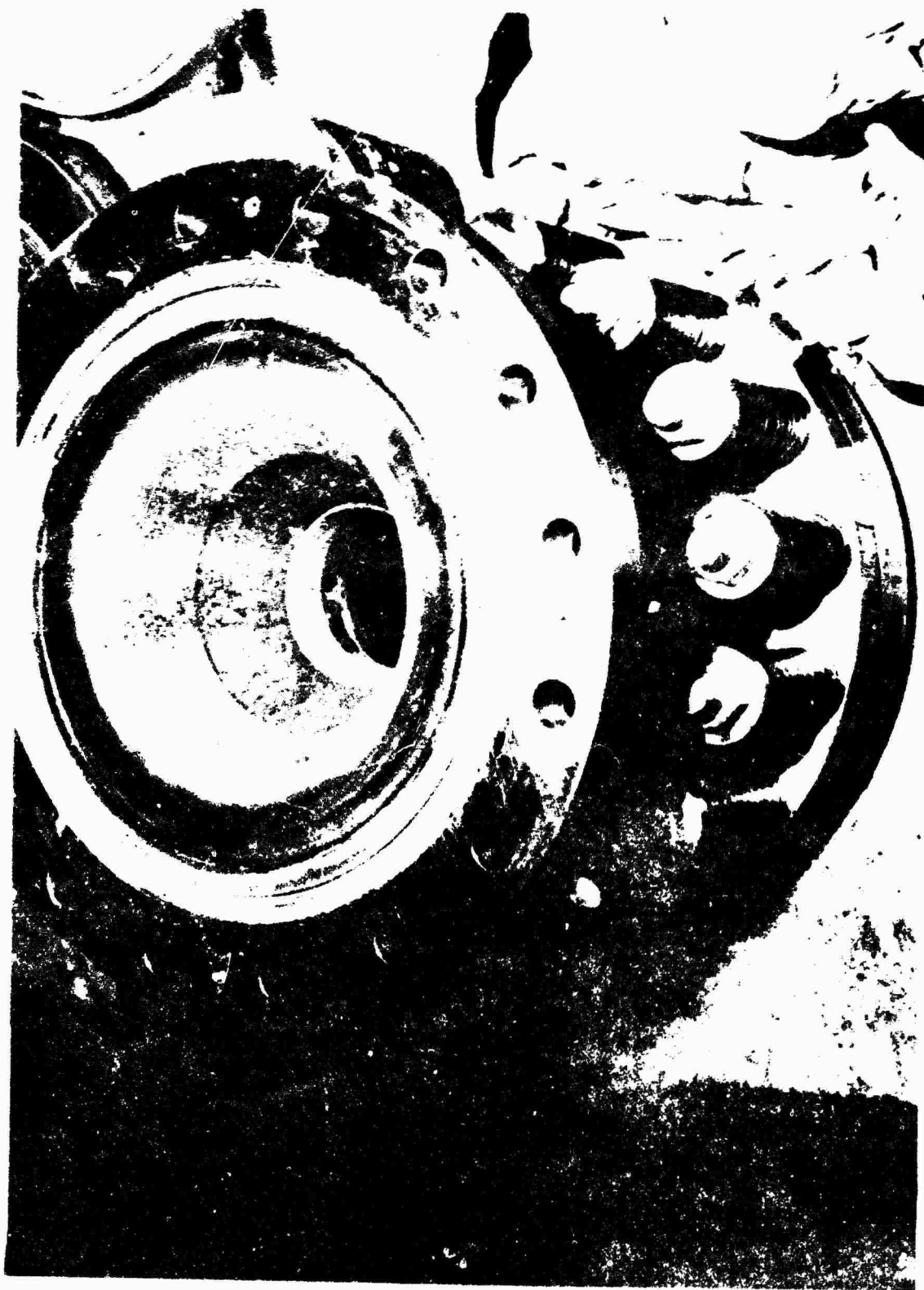FIGURE 18. ENTRANCE OF BORIDE NOZZLE NO. 2 AFTER 25 SECOND FIRING
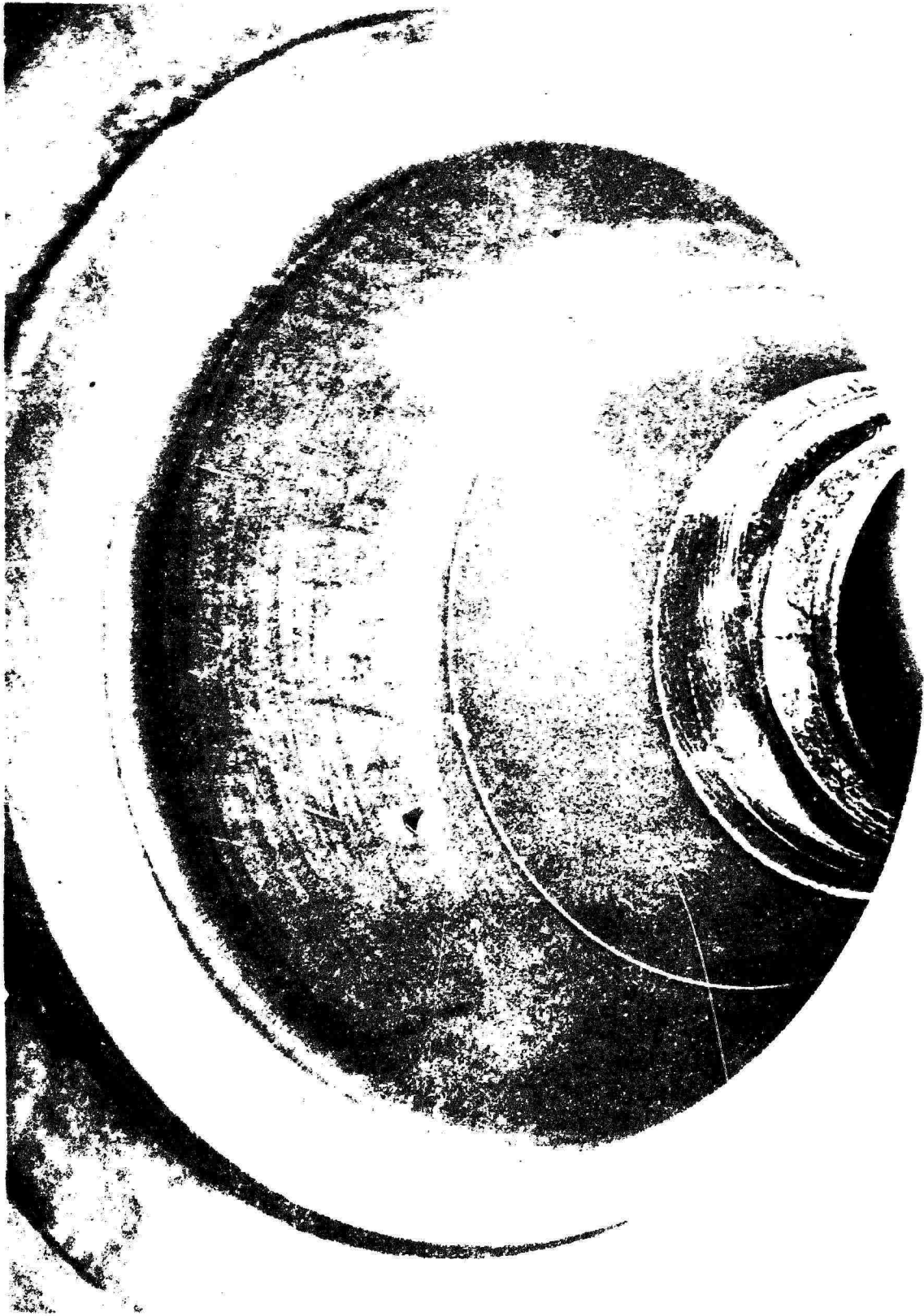
NEG C73-271-12

33

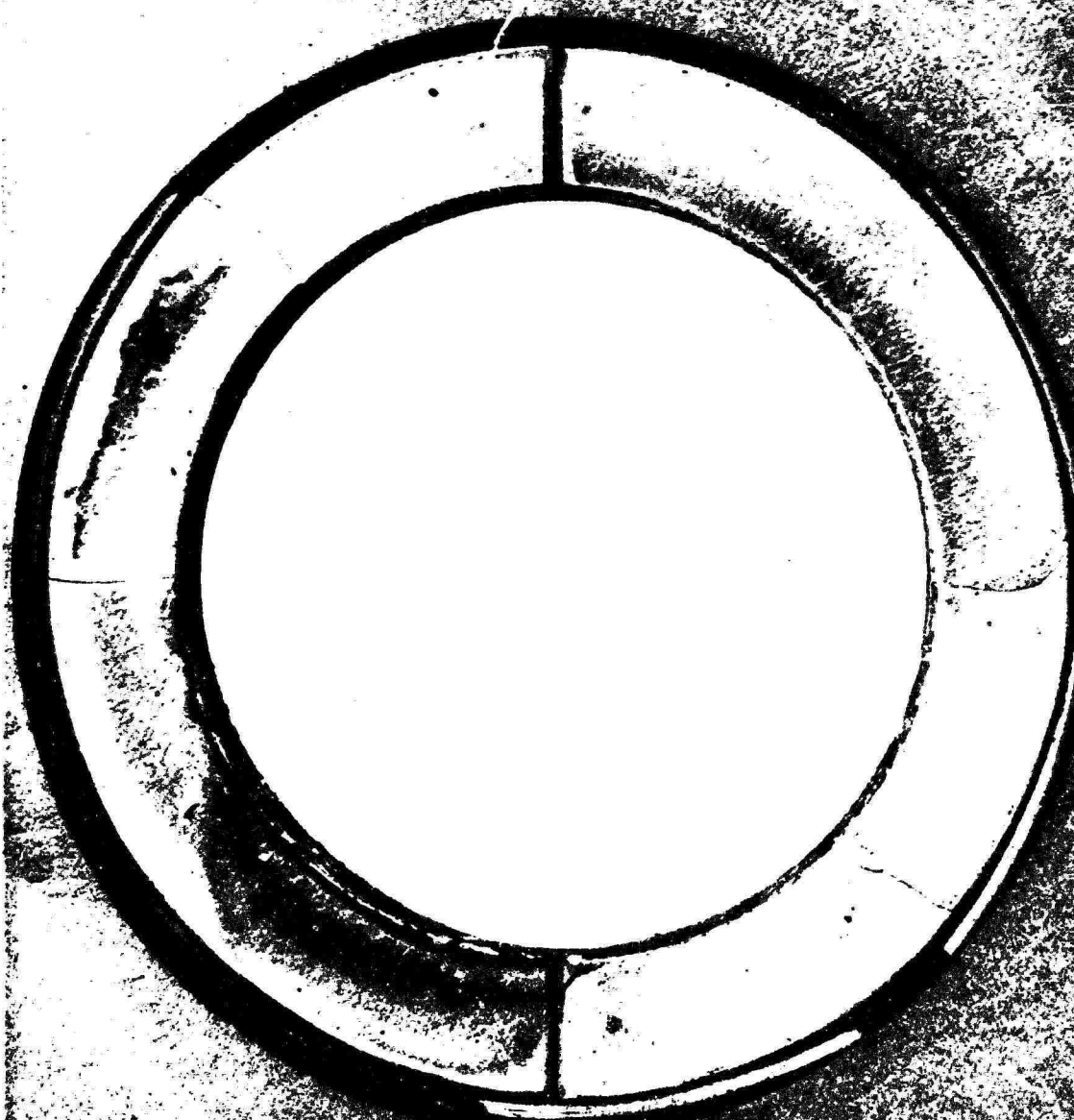FIGURE 19.   BORIDE NOZZLE NO. 2 AFTER 55 SECOND FIRING

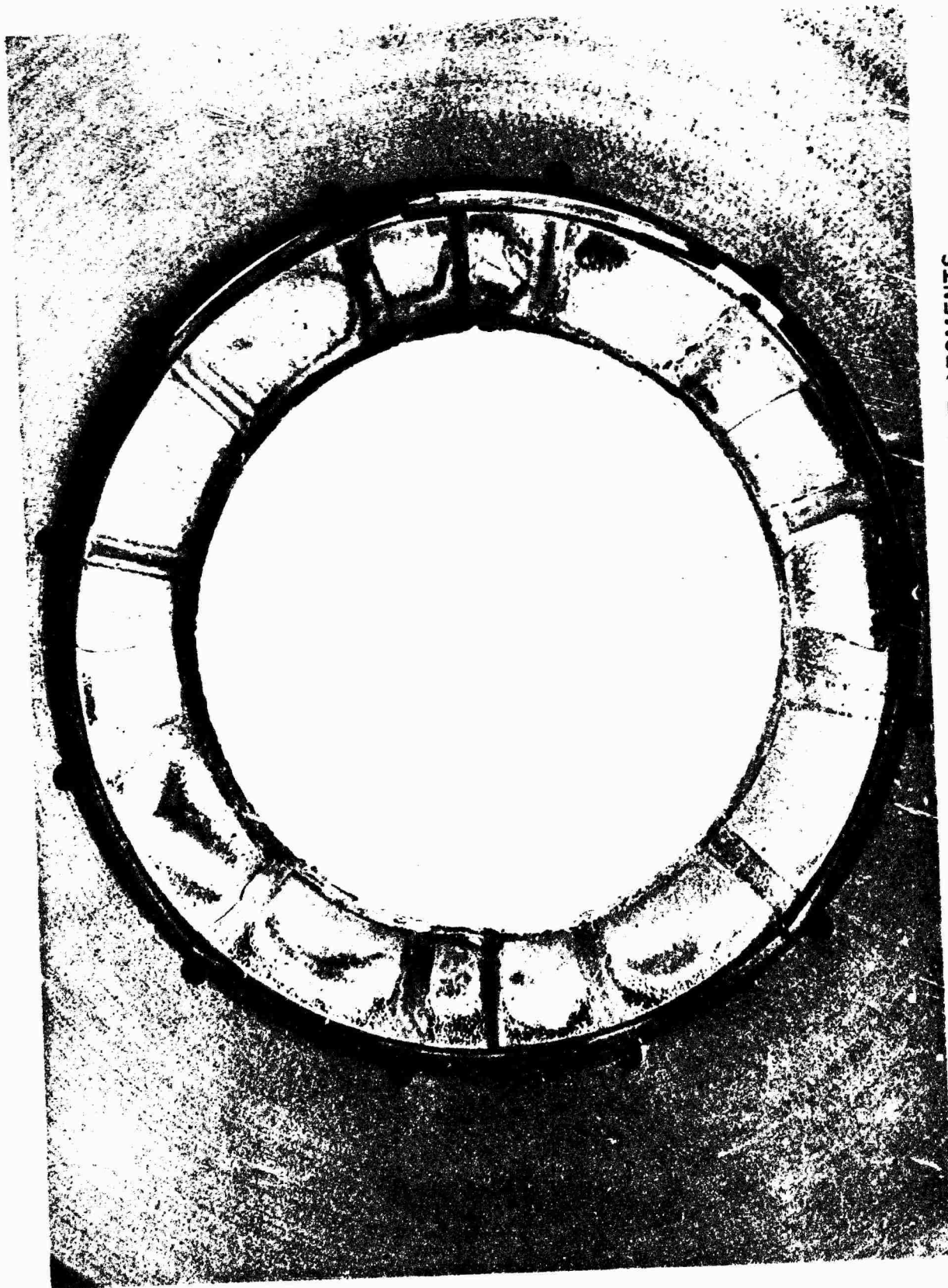FIGURE 20. SEGMENTED INSERT FOR BORIDE NOZZLE NO. 2 AFTER FIRING

35

FIGURE 21. DOWNSTREAM SIDE OF BORIDE SEGMENTS

36

SECTION V

PYROLYTIC GRAPHITE/CARBITEX NOZZLE NO. 1

A pyrolytic graphite coated Carbitex 713 nozzle was fabricated with the design shown in Figure 22. The structural design and durability of a similar nozzle had previously been established during test firings with fluorinated propellants. The interest in a PG/Carbitex nozzle for the current program, which required oxidation-resistant rocket nozzles, was due to the results of test firings of pyrolytic graphite coated nozzle inserts in N_2O_4/N_2H_4 reported in Reference 3. The low erosion rates reported therein were difficult to explain in light of the available data on oxidation rates of pyrolytic graphite. Therefore, a pyrolytic graphite coated nozzle was included in the program with the primary objective of determining chemical erosion rates in a large nozzle with N_2O_4/N_2H_4 propellants. Such propellants, at a mixture ratio of 1.2, would produce a water vapor mole fraction of about .45. The predicted throat erosion rate at a wall temperature of 4000°F was about 0.3 mil/sec, which would be excessive for the contract objectives.

1. DESIGN AND FABRICATION

The nozzle assembly (Figure 22) was designed to provide a free-standing PG/Carbitex nozzle attached and sealed to the water cooled adapter by spring loading against Viton O-rings in the adapter. This required that the front edge of the Carbitex be smooth and free from delaminations or flaws, which would provide leak paths around the O-rings. When the final cut was made on the edge of the Carbitex chamber after application of the PG coating, deep grooved delaminations were found in the Carbitex. Electrodeposited nickel was then deposited on the front end of the chamber and machined to form a smooth, flat forward face of nickel to bear against the O-rings. The nickel flange and entrance of the nozzle is shown in Figure 23.

There were a number of circumferential surface flaws in the entrance region of the Carbitex, which caused clusters of pyrolytic graphite nodule growth. The throat region was quite smooth, without any flaws in the Carbitex or nodule clusters in the pyrolytic graphite coating.

The Carbitex 713 nozzle, made by Carborundum Co., was coated with 0.100 inch thick pyrolytic graphite by Super Temp Co. The electrodeposited nickel was applied by Electroforms, Inc., Gardena, California. The length of the PG/Carbitex nozzle was cut so that it would be just contacting the rear Speer graphite ring after application of the spring preload. Therefore, as the nozzle heated up, the bearing load on the nickel flange would increase, thereby insuring minimum contact resistance between the nickel flange and the water cooled adapter to avoid melting of the nickel flange.
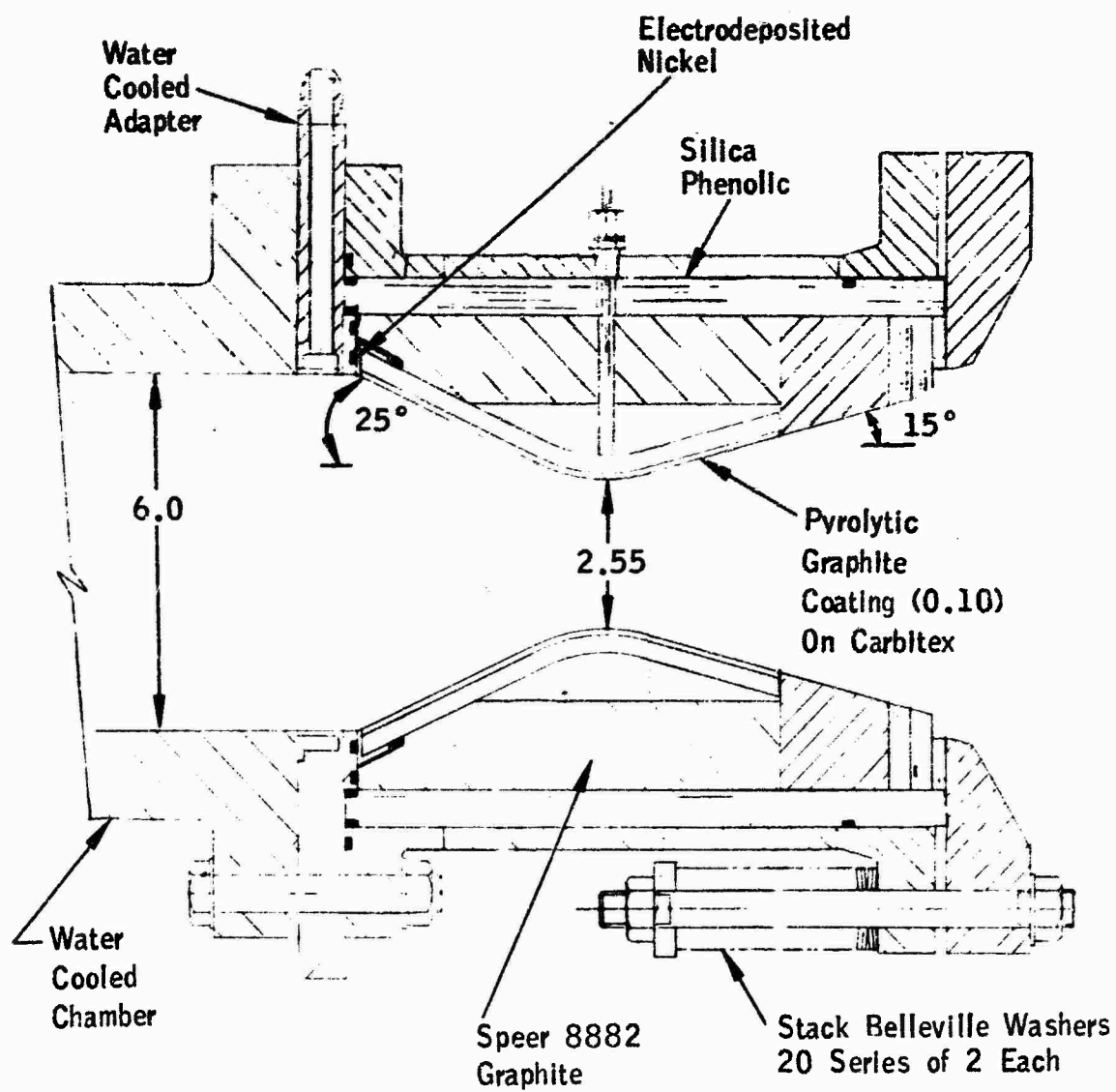
FIGURE 22. DESIGN OF PYROLYTIC GRAPHITE/CARBITEX/ NOZZLE NO. 1
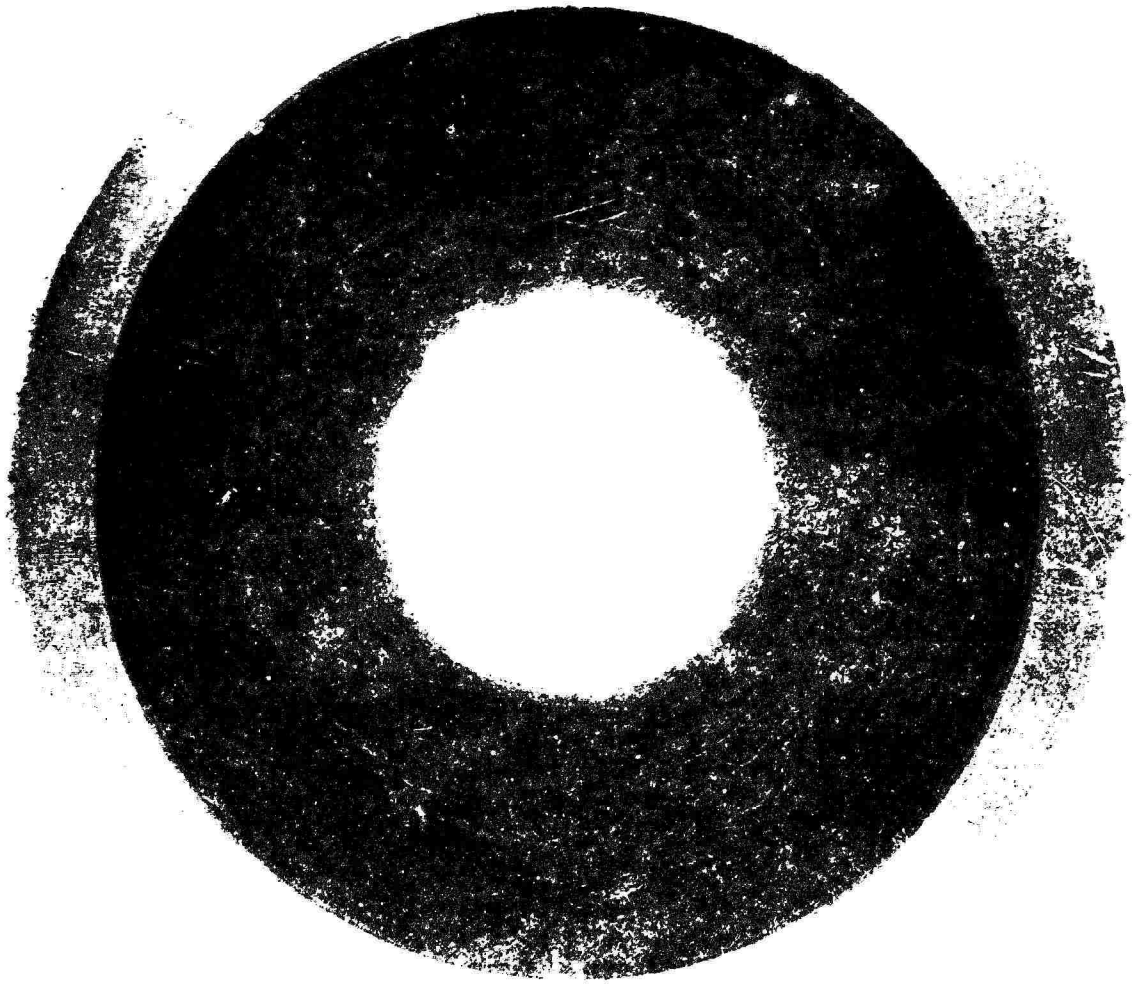
FIGURE 23. ENTRANCE OF PG/CARBITEX NOZZLE NO. 1

2. TEST FIRING EVALUATION

The PG/Carbitex Nozzle No. 1 was test fired at AFRPL on 1 June 1972 with N_2O_4/N_2H_4 at a mixture ratio of 1.14. The nozzle failed 20 seconds after ignition. The chamber pressure had dropped slightly from a mean value of about 360 psig to 352 psig at the time of failure.

A post test examination of the nozzle showed that the PG/Carbitex nozzle had been completely removed. Only a small portion of the Carbitex at the beginning of the contraction region, held by the Speer graphite support, was still in place. The nickel ring, which had been electrodeposited on the leading edge of the PG/Carbitex nozzle insert to seal off a delamination in the Carbitex, showed no sign of overheating. The most likely cause of failure was thought to be an excessive axial load, due to restraint of thermal expansion of the PG/Carbitex, possibly combined with residual stress concentrations along the circumferential nodule clusters in the nozzle entrance.

A second possible cause of failure was excessive erosion in the convergent region, because the amount of oxidation in the convergent region almost always exceeds that in the throat, since chemical erosion of such pyrolytic graphite chambers is approximately proportional to static pressure, if other conditions such as temperature and reactive specifies concentration are equal.

Subsequent examination of the chamber pressure oscillograph trace showed that combustion instability had occurred during the firing, with ± 50 psi oscillations at 80 to 90 cps. The C* efficiency was only 77.3 percent.

Since the frequency of instability was relatively low, the full amplitude of chamber pressure rise was within recording capability of the oscillograph, so that peak chamber pressures should not have exceeded about 425 psia. The nozzle had been designed for 400 psia. An analysis of dynamic loading on the chamber structure was not done so that the importance of the combustion instability on the nozzle failure cannot be accurately estimated.

SECTION VI

PYROLYTIC GRAPHITE/CARBITEX NOZZLE NO. 2

1. DESIGN AND FABRICATION

The 20 second firing of Pyrolytic Graphite Nozzle No. 1 had not been sufficient to determine nozzle erosion rates at steady state temperatures. Therefore, another nozzle and a new water cooled adapter were fabricated with the design configuration shown in Figure 24 . This design eliminated any problem of sealing between the Carbitex 713 and the water cooled adapter, but had the disadvantage of creating a turbulent region downstream of the water cooled adapter which could cause higher oxidation rates there or in the throat. Furthermore, any film cooling provided by the injector would be essentially eliminated, causing a higher film temperature along the nozzle wall than for Pyrolytic Graphite Carbitex Nozzle No. 1. A very good quality coating was deposited in the nozzle entrance and throat, as shown in Figure 25 . Only one large nodule developed during deposition. Several circumferential flaw lines in the Carbitex throat were coated over with PG, and the flaw lines were barely visible.

The coating in the exit was much less satisfactory, with many nodules caused by surface flaws in the Carbitex.

The coating thickness deposited by Super Temp Co. was only 0.085 inch instead of the design value of 0.100 inch, due to some unexplained difference in deposition rates from that of Pyrolytic Graphite Nozzle No. 1.

A second injector, essentially the same design as the first injector, was found to be free of combustion instability, and was used for subsequent tests.

2. TEST FIRING EVALUATION

The nozzle was given a 15 second firing using N_2O_4/N_2H_4 at a mixture ratio of 0.94. The C^* efficiency was 86.2 percent. The nozzle was examined after the firing while still mounted on the thrust stand. The nozzle was in excellent condition, with only slight throat erosion of about 0.010 inch. Chamber pressure had dropped about 15 psi during the run.

Any erosion which might have occurred in the entrance region could not be measured with the nozzle on the thrust stand.

A second firing of 40 seconds was then made, during which another 15 psi drop in chamber pressure occurred. It had been previously estimated that about 50 mils of pyrolytic graphite erosion would be the maximum allowable because of structural requirements. Therefore, the run was terminated after a total of 30 psi drop in chamber pressure had occurred.

41
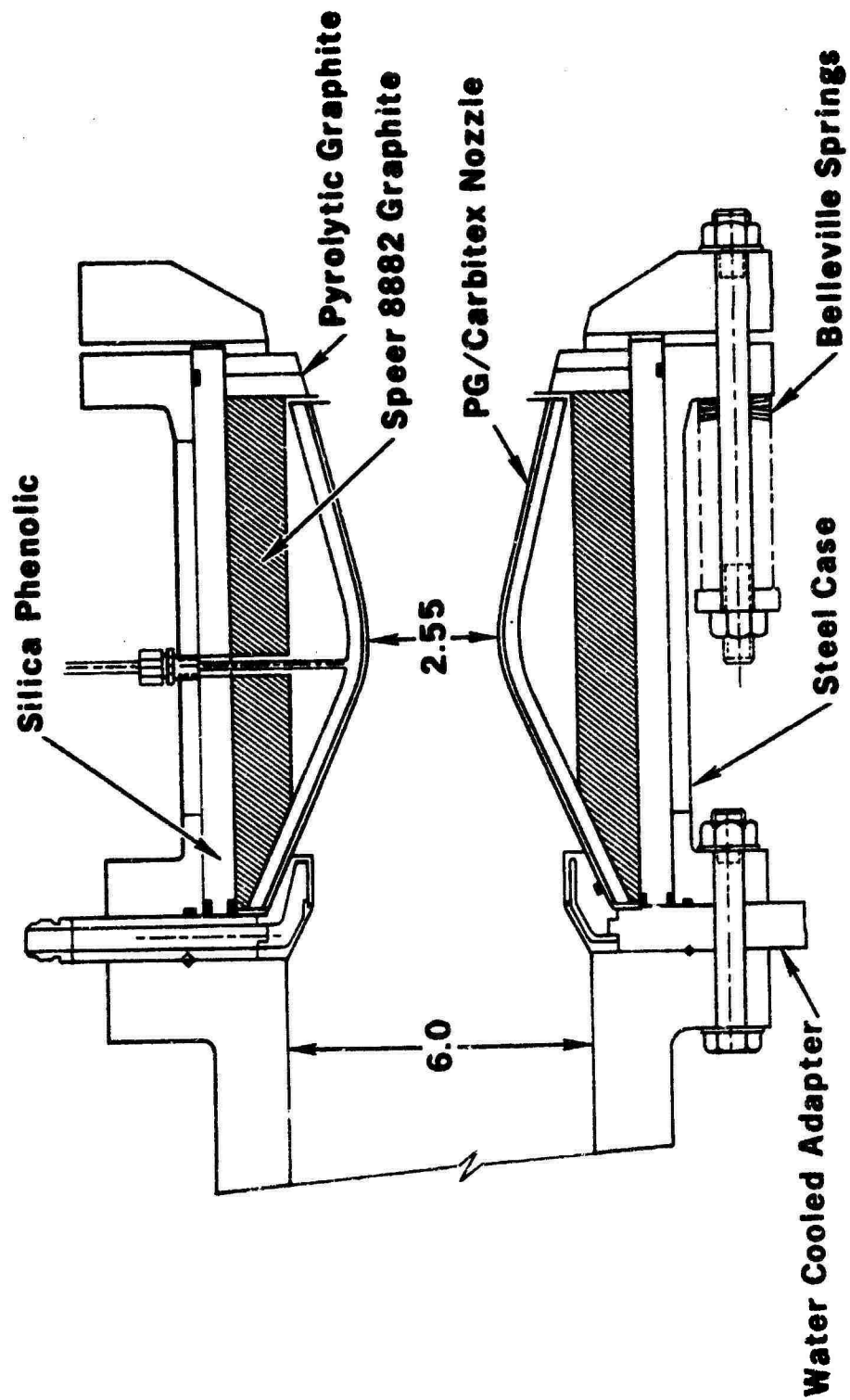
FIGURE 24.   DESIGN OF PYROLYTIC GRAPHITE/CARBITEX NOZZLE NO. 2

The figure is labeled with:
- Silica Phenolic
- Pyrolytic Graphite
- Speer 8882 Graphite
- PG/Carbitex Nozzle
- Belleville Springs
- Steel Case
- Water Cooled Adapter
- 2.55
- 6.0
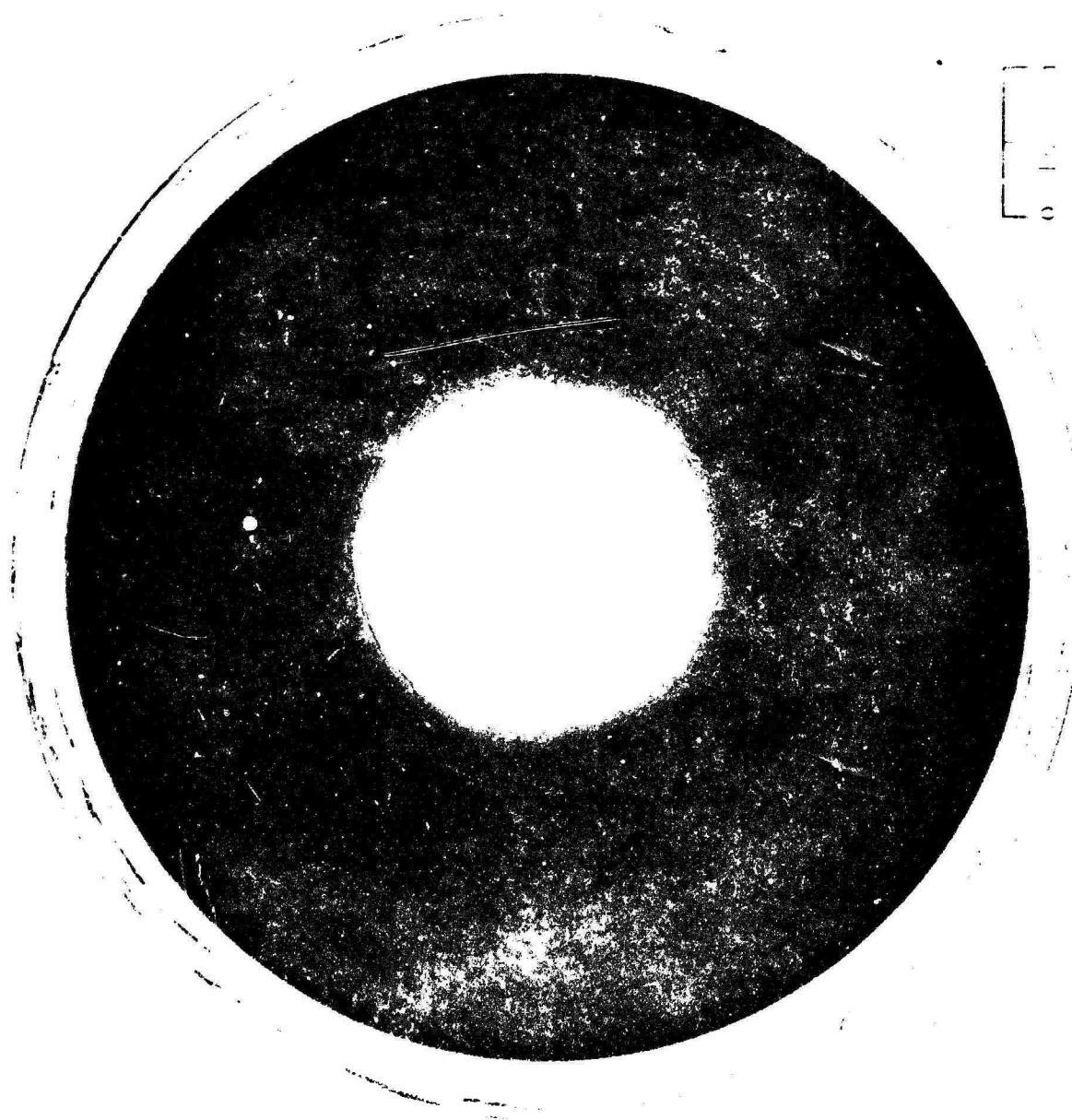
FIGURE 25. ENTRANCE OF PG/CARBITEX NOZZLE NO. 2

The nozzle was in good condition after the firing except that the nozzle had broken downstream of the water cooled adapter with a circumferential crack. The pyrolytic graphite coating thickness at this location was measured to be as thin as 0.040 inch, with some circumferential variation up to about 0.060 inch.

The entrance of the nozzle after firing is shown in Figure 26. The single large nodule had not caused any structural problem, although erosion around it was greater than elsewhere.

The throat erosion was uneven, with the greatest enlargement in the vicinity of the circumferential line flaws. The entire nozzle was still coated with pyrolytic graphite, and there was no evidence of separation of the pyrolytic graphite from the Carbitex. The maximum erosion was about 0.052 inch. Elsewhere the throat erosion was about 0.032 inch and quite uniform.

It was concluded that nominal throat erosion rates of the pyrolytic graphite coating were approximately 0.6 mils/sec. These erosion rates are considered typical and to be expected using N_2O_4/Amine propellants without film cooling. Lower erosion rates could be expected with film cooling or mixture ratio stratification. The maximum localized erosion rate was about 1.0 mils/sec.

These tests demonstrated the excellent thermal expansion compatibility and coating adherence between Carbitex 713 and the pyrolytic graphite coating. As in earlier thrust chamber tests, surface flaws in the Carbitex 713 were present and detracted from the structural strength and erosion resistance of the PG/Carbitex. Application of this material system as a throat insert rather than as primary structure would alleviate some of the effects of Carbitex surface flaws.
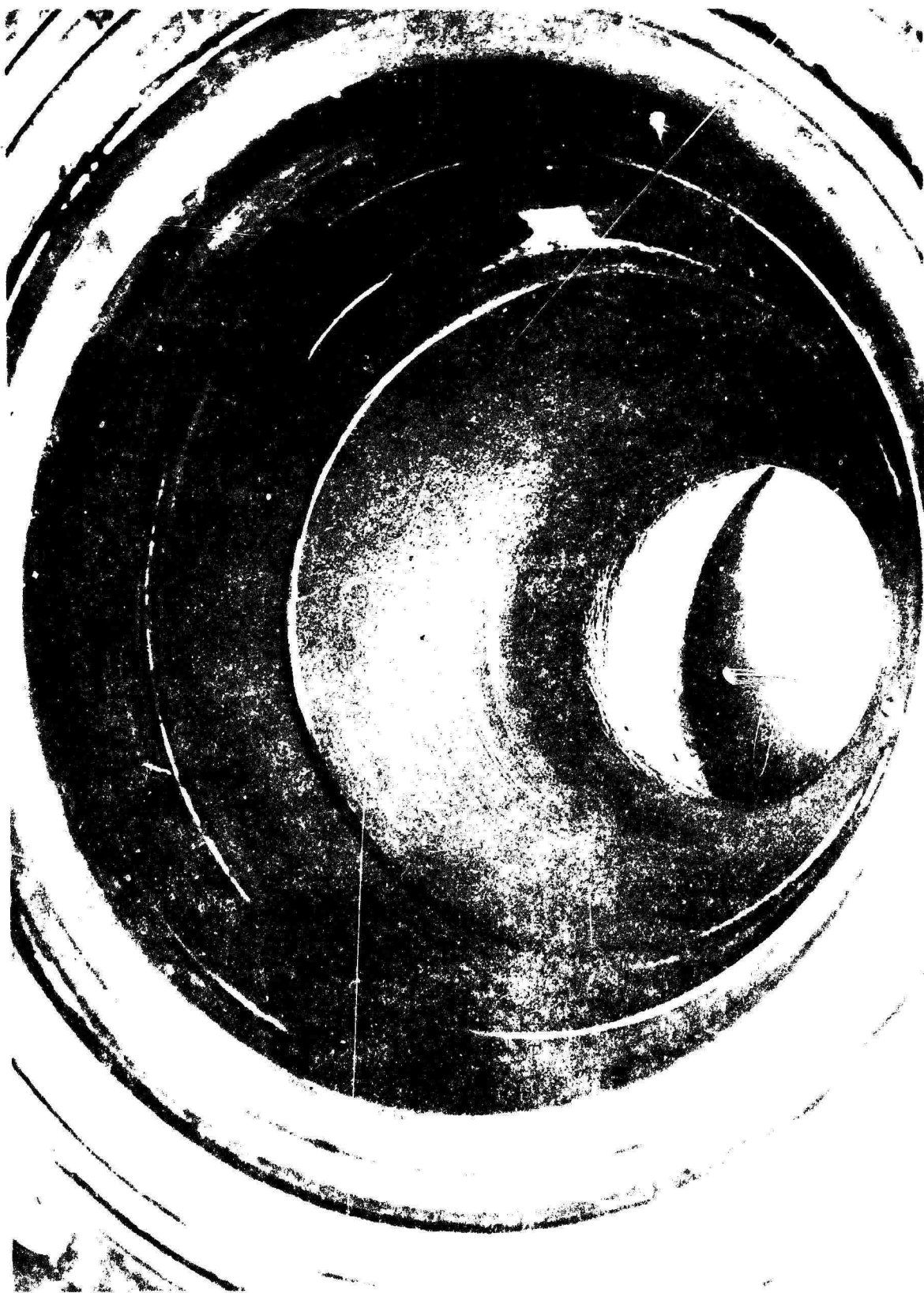
FIGURE 26. ENTRANCE OF PG/CARBITEX NOZZLE NO. 2 AFTER FIRING

SECTION VII

PYROBOND NOZZLES

Three PYROBOND nozzles made of filament wound graphite yarn with a CVD carbon matrix were fabricated with the design goal of being interchangeable with the Carbitex nozzles. Because of program redirection, this effort was terminated before completion of fabrication. The three filament windings shown in Figure 27 were wound by the Whittaker Corporation, San Diego, California, using Hitco GY2-1 yarn.

The winding pattern was changed after Nozzle No. 1 had been wound in order to get a closer fiber spacing in the large diameter portions of the nozzles.

The nozzles were infiltrated with CVD carbon by Super Temp Co. The entrance of Nozzle No. 2 is shown in Figure 28 after infiltration. A side view of Nozzle No. 2 is shown in Figure 29 . Material at both ends of the nozzle as shown would be removed in final machining to the design length.

The quality of the three nozzles varied. with No. 2 nozzle showing the best yarn spacing uniformity and infiltrated surface smoothness.
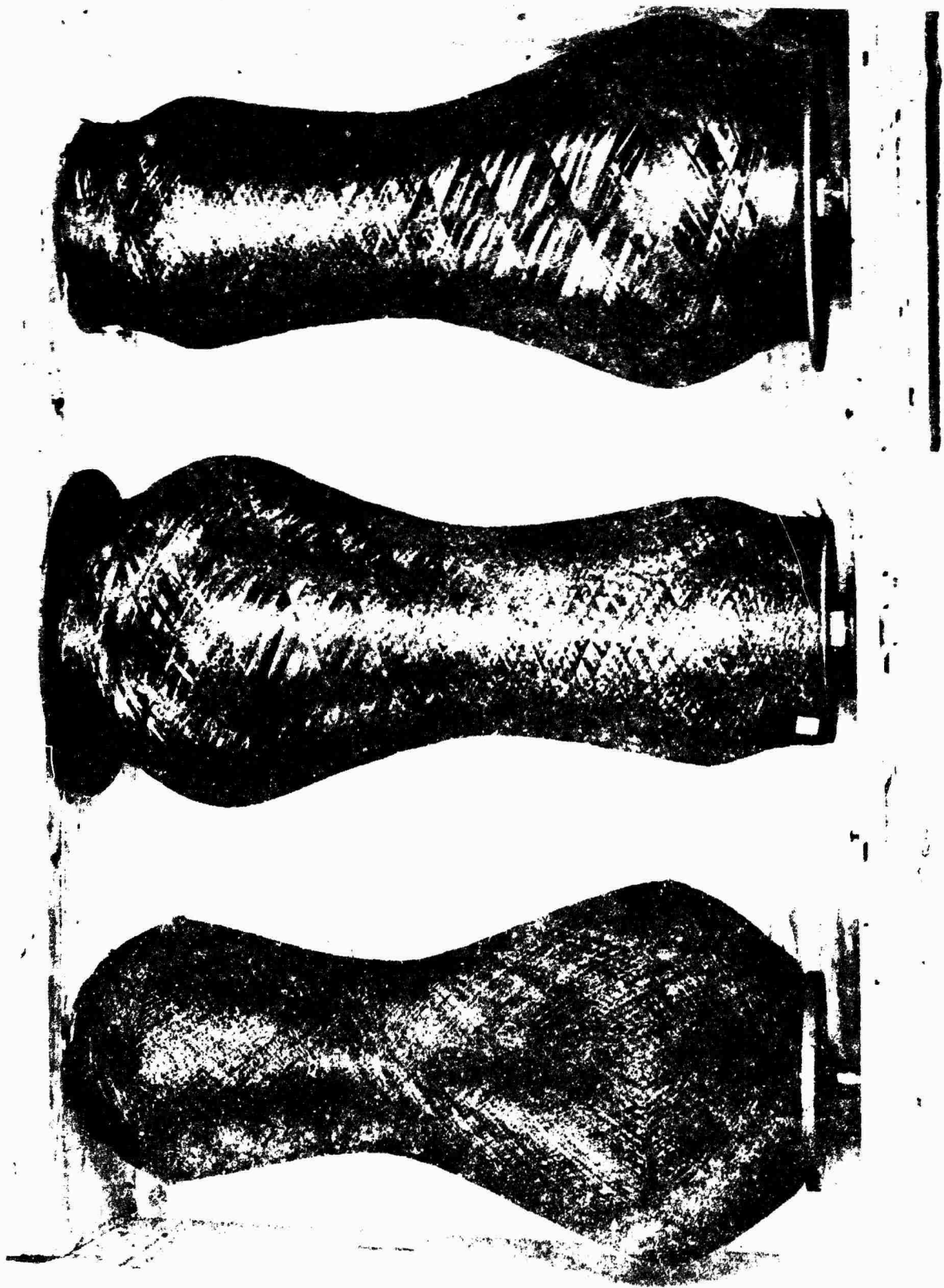
FIGURE 27. FILAMENT WINDINGS FOR PYROBOND NOZZLES

FIGURE 28. PYROBOND NOZZLE NO. 2 ENTRANCE

FIGURE 29. PYROBOND NOZZLE NO. 2 SIDE VIEW

inches

0 1 2 3

SECTION VIII

ZIRCONIUM CARBIDE/PYROLYTIC GRAPHITE/CARBITEX NOZZLE

One of the types of nozzles selected for this program consisted of a Carbitex 713 liner coated with a pyrolytic graphite alloy containing either zirconium carbide or hafnium carbide. Preliminary fabrication studies with coatings on 2 inch diameter Carbitex 713 tubes were successful, and fabrication of a zirconium carbide/pyrolytic graphite coated Carbitex nozzle was begun. All of the ZrC/PG and HfC/PG deposition work was done by the Raytheon Company, Waltham, Mass. This fabrication was not completed because of program redirection to concentrate on carbide/pyrolytic graphite washer nozzles.

1.   TUBES

Two Carbitex 713 tubes and two PYROBOND tubes, approximately 2 inches in diameter, were coated on the inside with carbide/pyrolytic graphite alloys as listed in Table IV . The PYROBOND tubes were made by Super Temp Company.

TABLE IV

CARBIDE/PYROLYTIC GRAPHITE COATED TUBES

Run No.	Pyrolytic Coating	Tube Length	Coating Thickness	Wt. Percent of Metal	Graphitic Tube
MQP-109	ZrC/PG	4.68	0.060	25	Carbitex 713
MQP-110	ZrC/PG	2.0	0.100	25	GSGY2-5 Pyrobond
MQP-112	HfC/PG	4.9	0.080	50	Carbitex 713
MQP-113	HfC/PG	2.0	0.080	50	CY2-1 Pyrobond

The ZrC/PG coating from Run MQP-109 was of excellent quality with no visible cracks or delaminations. The zirconium content ranged from 20 percent at the entrance to 30 percent at the exit.

The coating thickness on run MQP-110 was 0.100 inch instead of the intended 0.080 inch. Because of the large thickness-to-radius ratio approaching 0.10, there was a delamination within the ZrC/PG. However, the adherence of the coating to the PYROBOND tube appeared to be excellent.

The HfC/PG coatings on the last two runs appeared to be of excellent quality, with no cracks or delaminations. The interface and microstructure of the HfC/PG coating on the CY 2-1 PYROBOND tube is shown in Figure 30 . The HfC/PG coating appears to be anchored into the PYROBOND tube by deposition within the gaps between graphite yarns.

2.   NOZZLE FABRICATION

Two furnace runs were made by the Raytheon Company to deposit a 0.10 inch thick coating of ZrC/PG on the inside of Carbitex nozzles procured from the Carborundum Company. A metal content of 25 percent by weight was desired. Thermal stress analysis showed that this composite nozzle would be structurally satisfactory.

Dendritic growths occurred in both nozzles, but the coating microstructure, thickness and adhesion to the Carbitex was excellent in areas not affected by the growths.

The coating produced by the second furnace run is shown in Figure 31 . A third furnace run made with an ATJ graphite nozzle produced similar growths. Analysis of the flow rates and nozzle geometry led to the conclusion that the growths were caused by flow separation due to rapid area expansion and were unrelated to slight surface flaws on the Carbitex. It was expected that the problem of dendritic growth could be solved without much difficulty by proper design of a plug for control of flow expansion in the exit nozzle. However, this portion of the contract effort was discontinued after the third run because of program redirection.
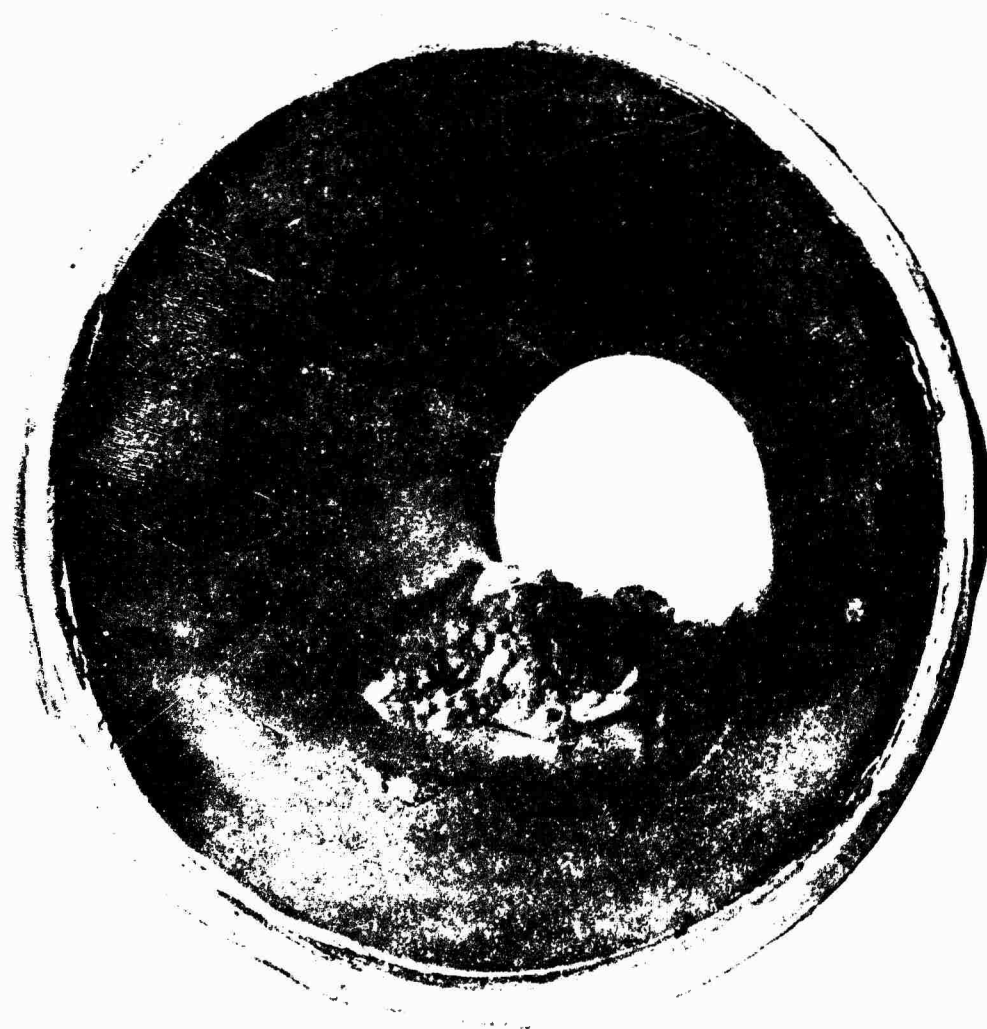
X 500

X 50

FIGURE 30. HfC/PG DEPOSIT ON PYROBOND

52

FIGURE 31. ZrC/PG COATED CARBITEX

SECTION IX

CARBIDE/PYROLYTIC GRAPHITE WASHER NOZZLE

One of the three types of nozzles chosen originally for this program was to be made of edge oriented washers of pyrolytic graphite alloys containing hafnium carbide or zirconium carbide. This material system had previously been successfully test fired at Marquardt with oxidizing propellants at a chamber pressure of 100 psia as reported in Reference 5 . These test firings exposed the c-plane edge of the washers to oxidation and gas shearing forces. The ZrC/PG and HfC/PG washers have many potential advantages over pure PG washers, including much superior oxidation resistance and lower axial thermal expansion. The previous test firings had shown very small throat erosion with test durations over 400 seconds. No stress failures or cracking occurred in the test firings. Oxidation resistance is due to the formation of an adherent surface coating of ZrO_2 or HfO_2 with oxide melting temperatures near 5000°F.

Pyrolytically formed alloys of zirconium carbide and hafnium carbide with graphite have been developed by Raytheon Company during recent years under a series of subcontracts to Marquardt funded by NASA. Results of this work are presented in References 5 and 6 . These material systems have melting temperatures above 5000°F, have tensile strengths between 20,000 and 40,000 psi at room temperature, and flexure strengths of 40,000 to 80,000 psi at temperatures up to 4000°F.

The carbide/pyrolytic graphite alloys have unique physical properties which set them apart from other carbide/graphite composites such as JTA graphite or arc cast carbide/graphite composites. In particular, the zirconium carbide and hafnium carbide are not coatings and are not granular, but are dispersed throughout the structure in such a fine alloy that the carbide phase cannot be detected by photomicrographs.

The zirconium carbide and hafnium carbide alloys in pyrolytic graphite are formed by simultaneous vapor deposition from a mixture of carbon source gas (methane) and a metal source gas (zirconium tetrachloride or hafnium tetrachloride). The process is shown schematically in Figure 32. The microstructure and physical properties of the ZrC/PG and HfC/PG alloys are similar to pyrolytic graphite in that the structure is completely impervious and the material has a degree of anisotropy, which decreases as metal content is increased.

1. FABRICATION

The largest flat plates of ZrC/PG or HfC/PG made by Raytheon prior to this program had been in three inch widths. Production of carbide/PG plates had been more difficult than production of unalloyed PG but plates up to 0.25 inch thickness had been made and used in the 100 lb. thrust nozzle firings. Therefore, Marquardt had predicted that production of six inch diameter plates of 1/4 to 3/8 inch thickness could be accomplished without too much difficulty. It was found during this program that this prediction had been incorrect, and a much larger effort than originally envisioned was made in an attempt to make HfC/PG and ZrC/PG plates.

TO VACUUM PUMPS

PORT FOR
OPTICAL TEMPERATURE
MEASUREMENT

GRAPHITE TUBE MANDREL

PG FURNACE

PYROLYTIC CARBIDE DEPOSITION

GRAPHITE HEATING ELEMENT

NOZZLE COOLING WATER

CH_4 METERED FLOW

PURE METAL CHIPS (Zr or Hf)

CHEMICAL VAPORIZER

HEATER ELEMENT

$(Cl_2 + A)$ GAS METERED FLOW
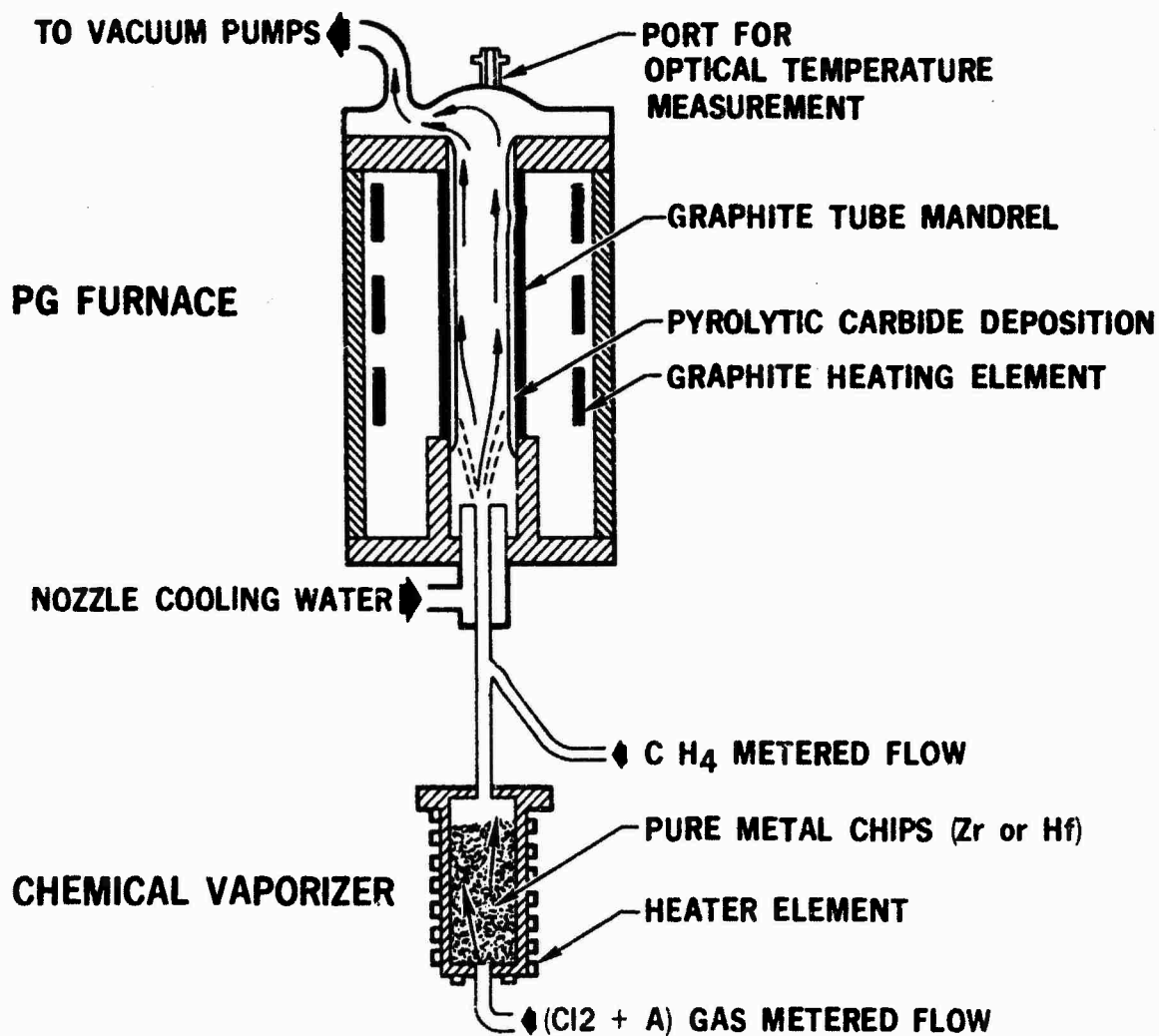
V4946-15

FIGURE 32. SCHEMATIC OF DEPOSITION FURNACE AND CHEMICAL VAPORIZER

55

Hafnium pyrocarbide (HfC/PG) and zirconium pyrocarbide (ZrC/PG) are made by Raytheon Co. using a mixture of $HfCl_4$ of $ZrCl_4$ and methane injected into a vacuum furnace, where pyrolysis takes place, followed by vapor deposition of PG and the carbide. The injector, usually located near the bottom of the furnace, is exposed to radiation heat transfer from the furnace, and must therefore be water cooled. On the other hand, the metal chlorides condense inside the injector unless the injector is heated above their sublimation temperatures, 331°C for $ZrCl_4$, or 317°C for $HfCl_4$ at 1 atmosphere.

The microstructure and general physical properties of the pyrocarbides are similar to those of pyrolytic graphite. However, some of the properties, although similar in kind, differ in magnitude. These differences are not of significance when making axisymetric depositions, as evidenced by the successful fabrication of large numbers of thrust chambers, as reported in References 5 and 6. However, the differences between unalloyed PG and the carbide alloys do create much more difficulty in making flat plates.

The first problem encountered in making flat plates of carbide/pyrolytic graphite alloys is due to the need for longer furnace runs than when making axisymetric deposits, which are generally thinner than the desired plate thicknesses of 1/4 to 3/8 inch. This aggravates a problem of injector plugging when depositing the carbide alloys, which is not a problem in making pyrolytic graphite. The carbide alloys form hard, adherent deposits over the tip of the injector, which can eventually block all gas flow and terminate the run.

A second problem encountered in making pyrocarbides is the fact that their deposits on open shapes such as mandrels for flat plates have a greater tendency to bow and delaminate than do deposits of pyrolytic graphite. The complex interactions of anisotropy, variable lattice transformation, and plastic deformation of pyrolytic graphite is not well understood. The property causing the major difficulty in pyrocarbide plate fabrication is thought to be "growth", or variable lattice transformation, which produces a permanent growth in the a-direction and shrinkage in the c-direction upon exposure to elevated temperatures. An empirical treatment of these factors has been found for fabrication of pyrolytic graphite plate. Flat PG is ordinarily made from bowed plates, the result of residual stresses caused by interaction of the material phenomena mentioned above. It was hoped that a empirical treatment of these factors would also be successfull for fabrication of pyrocarbide plate.

Raytheon made a total of 25 furnace runs to fabricate material for ZrC/PG or HfC/PG washers during this program. The run data are summarized in Table V .

The argon flow through the metal retort was added to the Cl_2 flow to get better mixing in the retort, where the Cl_2 reacts with heated metal chips to produce the metal chloride. Some hydrogen flow was mixed with the methane flow in a few early runs. The argon flow through the injector tip was used to protect the injector tip from source gases. During early runs using a Raytheon injector, this argon flow was injected through separate tubes into the area around the injector tip. The argon flow was later injected through an injector tip designed by Marquardt.

TABLE V

RUN SUMMARY - FLAT PLATE FABRICATION - ZrC/PG AND HfC/PG

Run No.	Temp. °C	Press. mm Hg	Run Time Hrs	CH₄	A Retort	Cl₂	H₂	A Tip	Total	Deposit Thk. in	Deposit Rate Mils/hr	Flow Arg in	Unit Flow Rate liters/ in²min	Mandrel Setup	Injector	Comments
MQZP-81	1825	15	10	4	.5	.55	4.		9.05					6 x 6 box, 18" long Straight flow	Raytheon	Injector plugged around baffle
MQZP-82	1675	15	23	2	.5	.4	2.		4.9					Same	Raytheon	Same
MQZP-83	1825	15	21	2	.5	.3	.5		3.3					3 port box Reverse flow	Raytheon	Injector plugged thin sooty deposit
MQZP-84	1700	5	8	6	.5	.2	-		6.7					4 port box Reverse flow	Raytheon	Injector plugged
MQZP-85	1700	5	21	6	1.	.2	-		7.2					4 port box Reverse flow	Raytheon	Injector plugged
MZQP-86	1700	5	48	6	1.	.2	-		7.2			35		2 port box, 4 1/2 x 6" mandrels flat and circular straight flow	Raytheon	No injector plugging
MQZP-87	2100	5	17	6	1.	.2	-		7.2	30-40	2.0	56	.78	Two 4 port boxes in series flat circular mandrels straight flow	Raytheon	Injector plugged thin deposits in top box
MQZP-88	2050	10	8	6	1.	.2	-	1.8	9.					2 port box - 2 sides curved plate straight flow	Raytheon	Plugged in line, elect. failure. Plates from curved mandrel came off flat
MQZP-89	2000	15	36	6	.5	.2	-	1.8	8.5			56		4 port box, curved mandrels straight flow	Raytheon	Injector plugged. No data on material
MQZP-90	1950	10	16	6	.5	.05	.5							4 sided plate box, curved sides, R = 3"	Raytheon small I.D.	Injector plugged
MQZP-91	1700	10	2	6	.5	.2	5 (H₂)							Marquardt copper	copper	Copper injector melted

57

TABLE V (CONTINUED)

RUN SUMMARY - FLAT PLATE FABRICATION - ZrC/PG AND HfC/PG

Run No.	Temp. °C	Press. mm Hg	Run Time Hrs	CH_4	A Retort	Cl_2	B_2	Tip	Total	Deposit Thick. in	Deposit Rate mil/hr	Flow Area in^2	Unit Flow Rate liters/in^2 min	Mandrel Setup	Metal (%)	Injector	Comments
MQZP-92	1700	10	18	6	.5	.2	-		-	.125		36		4 sided box 12" long, straight flow, 6 x 6 cross section, flat mandrel	Zr 1.5 t 3.5b	Raytheon small I.D.	Mat'l bowed, thin. No data or material available
MQZP-93	1700	10	4	6	.5	.2		5						6 x 6 box	Zr	Marquardt nickel	Clean nickel tip
MQZP-94	1675	5.0	20	6	.5	.1	-	5	11.6	.050	2.5			4 sided box, R = 19, 21, 23, flat reverse flow	Zr 1.75	Marquardt nickel	Box exits plugged No injec. plugging
MQZP-95	2150	5	21	6	.5	.1		2.5	9.1	.060b .088 t	2.9b 4.2t	36	.25	4 sided box, flat plates 6 x 6 x 12" long, straight flow	Zr 1.5	Marquardt nickel	Cl_2 supply plugged Ni tip clear, thin deposit. No injector plugging
MQZP-96	2150	7.5	40	6	.5	.1		5.	11.6	.120b .240t	3. b 6. t	36	.25	Same	Zr 1.5	Marquardt nickel	No plugging, good run
MQZP-97	1700	5	36	6	.2	.2		5.	11.4	.160a .250m	4.5	15	.77	2 boxes, 2 port boiler ea. box, 7 1/2 x 2 flow area, 1 ea. flat, 1 concave mandrel, R-60 sight, flow	Zr 16.5	Marquardt nickel	Good run. Deposits uneven thickness, Furnace elect. short
MQZP-98	2150	7.5	10	6	.5	.5		5	12	.036a	3.6	36	.33	2 boxes 6 x 6 straight flow	Zr 3.	Marquardt nickel	Injector plugged
MQZP-99	1700	5.0	40	6	.5	.2		6	12.7	.200a	5.0a	18	.70	2 boxes, 3 x 6 straight flow	Zr 8.2	Marquardt nickel	Cl_2 supply plugged, ma'l uneven thick., delaminated, bowed; tip partly plugged
MQZP-100	1500	5.0	50	6	.5	.2		6	12.7	.140b .120t	2.8a	18	.70	3 x 6 x 12 box, flat mandrels, st. flow 15.1n 13.2t	Zr 13.8	Marquardt nickel	Good run. No. inj. plug, ma'l uneven thick. delaminated

TABLE V (CONTINUED)

RUN SUMMARY - FLAT PLATE FABRICATION - ZrC/PG AND HfC/PG

Run No.	Temp. °C	Press. mm Hg	Run Time Hrs	CH₄	A Retort	Cl₂	A Tip	H₂ Total	Deposit Thickness in.	Deposit Rate mil/hr	Flow Area in.²	Unit Flow Rate liters/ in.² min.	Mandrel Setup	Metal (g)	Injector	Comments
MQZP-101	1400	5.0	38	6	.5	.2	6	12.7	.020	.5	18	.70	3 x 4 x 12 box flat mandrels straight flow	Zr	Marquardt nickel	Furnace abort. Thin deposit, delaminated
MQHP-102	1500	5	40		.5	.4	6	12.9	.090	2.2	18	.72	3 x 6 x 12 box flat mandrels straight flow	24b 36m 46t Hf	Marquardt nickel	No plugging. Mat'l badly delaminated. 10hr PG flash gave 0.018"
MQHP-103	1600	10	20	12	1.0	.8	6	19.8	.100	5.0	25	1.03	5 x 5 x 10 box flat mandrels straight flow	41.7b 39.2m 32.9t Hf	Marquardt nickel	Injector tip clean. One delamination in middle, perhaps due to furnace abort. 10 hr PG flash coat 0.030"
MQZP-104	1600	10	25	12.	1.	1.5	6.	20.5	.2	8	10		Two 2 x 5 boxes, flat mandrels straight flow	Zr 34, 43 36, 38	Marquardt nickel	10 hr PG precoat. Delaminated. No injector plugging
MQHP-105	1600	10	26.5	12.	1.	1.5	6.	20.5	.25	9.4	12.5		Two 2 1/2 x 5 boxes, flat mandrels straight flow	Hf 65	Marquardt nickel	10 hr PG precoat. Deposit bowed inward and cracked convolutions. Lid delaminated. Methane line plugged

a.   Runs 81 thru 90

A Raytheon injector was used for the first ten runs. The principal problem during these runs was plugging of the injector. A variety of furnace setup configurations were used in attempts to avoid plugging. On Runs 81 and 82, a conical expansion shroud was place around the injector, which had an O.D. of 1.5 inches. The conical shroud expanded from the injector O.D. to a diameter of 3.875 inches over a distance of 3 inches. The injector plugged in 10 hours on Run 81 and 23 hours on Run 82. An extension tube was placed on the injector for Run 83, but plugged in 21 hours. A graphite plate with a 1.5 inch diameter hole was placed just downstream of the injector on Run 84. However, the injector plugged in 8 hours. A similar design using a pyrolytic graphite plate plugged on Run 85 after 21 hours. On Run 86, the injector was inserted into a 3 inch diameter tube which, in turn, entered the mandrel volume. This run lasted 48 hours without plugging the injector.

The mandrels for Runs 81 and 82 were in the form of a 4-sided box, 18 inches long and square cross section of 6 x 6 inches. The source gases passed inside the box and deposited on the inside surfaces of the graphite plates forming the box. The deposits on these mandrels were very thin, partly because of the short run times. The sides were machined concave in the transverse direction with a radius of curvature of 20 inches, in an attempt to counteract plate bowing.

Circular depressed ports in the sides of the mandrel boxes were used on Runs 83 through 89. The circular depressions were 6 inches in diameter. In some cases, the source gas passed straight through the box, and was diverted to all sides at the exit by a lid held 1 inch above the box. In other cases, the lid sat directly on the top of the box, and the source gases reversed within the box and flowed out exit holes in the bottom of the box. Two curved plates of about 0.180 inch thickness were obtained from Run 86. The metal content at the center of the curved plate was 21.7 weight percent zirconium.

b.   Marquardt Injectors

After completion of Run 90, it was evident that injector plugging was a serious problem which would have to be solved if thick pyrocarbide plates were to be made. Therefore, Marquardt designed and fabricated two injectors with provision for injection of a concentric sheet of argon around the injector tip. The sheet of argon was intended to blanket the injector tip with a layer of inert gas so that the recirculating pyrolyzed CH_4 and metal tetrachloride could not deposit on the injector.

The first injector made by Marquardt had a copper tip. The copper tip melted during test Run 91. The second injector tip made by Marquardt had a Nickel tip and was tested successfully on Run 93. No deposits were found on the tip after a 4 hour run. This injector was used throughout the remainder of the program, and was fairly successful in eliminating injector plugging, although some plugging did occur on a few runs. The nickel tip injector is shown in Figure 33.
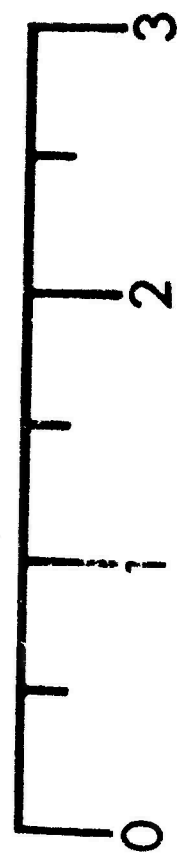
FIGURE 33. NICKEL TIP INJECTOR

c.   Runs 94 thru 99

Previous work by Raytheon had led to the conclusion that either a high temperature near 2150°C or a low temperature near 1700°C was preferred for making pyrocarbide plate. The low temperature was thought to be too low for rapid growth, while the high temperature was thought to accelerate the growth so that it would occur so soon after deposition that material deposited later would not be damaged.

Run 94 was a 20 hour run at 1675°C using a box mandrel with a recessed circular port mandrel in each of 4 sides. One mandrel was flat, and the other three were concave, with curvature radii of 19, 21 and 23 inches. The flow was reversed in the box, exiting out holes in the bottom. These exit holes plugged after 20 hours. The deposit was very thin (0.050 inch) and no significant advantage between the various mandrel curvatures could be seen.

Run 95 was made by Raytheon at 2150°C using straight flow through a box 12 inches long with 6 inch wide side⌐. The metal retort plugged after 12 hours, terminating the run. The material deposited on the side of the box was of excellent quality, but was found later to contain only 1.5 wt. percent zirconium. This result confirmed that production of PG plate is much easier than production of pyrocarbide plate containing significant amounts of carbide.

Run 96 was made with the same mandrel setup and furnace conditions as Run 95 and was terminated after 40 hours without any problems. The deposits on the mandrel sides varied from .120 inch at the bottom to .240 inch at the top. However, a much thicker plate was deposited on the lid, being about 0.4 inch thick with some bow. The lid had not been intended as a mandrel, but it was found that the deposit on the lid was not only thicker, but also had 11.2 wt. percent zirconium compared to only 1.5 percent on the side mandrels.

Run 97 was made with two box mandrels with a 7-1/2 x 2 inch cross-section. The reduced cross-section was used in order to get a higher Reynolds number, and presumably, higher deposit rates. A circular mandrel port was located in each of the 7-1/2 inch wide sides. Two such mandrel boxes were stacked in the furnace. The furnace temperature was 1700°C. The deposits in the mandrel were bowed and delaminated. The higher flow rate per unit area had produced greater deposition rates, however, about 4.5 mils/hr. The metal content of 15.5 percent was much higher than in previous runs.

Run 98 was made with the same furnace conditions as Run 96, except that the chlorine flow rate was increased five-fold in an attempt to get higher metal content. The injector plugged after 10 hours. The deposits on the mandrel sides were thin and contained only 3 percent zirconium. The deposit on the lid was sooty and cracked.

Run 99 was made at 1700°C in an attempt to avoid injector plugging and also to get higher metal content. The run was terminated after 40 hours by plugging of the metal retort. There was some deposit around the injector, but flow had not been blocked. A 3 x 6 inch cross-section was used in the mandrel box. Metal content was 8.2 percent and the deposition rate was 5 mils/hr. The deposited material was delaminated and bowed.

d.   Runs 100 thru 102

The next three runs were made at lower temperatures than ever before used, with the idea that growth at lower temperatures might be eliminated. It was also expected that injector plugging would be minimized and metal content would be increased at lower temperatures, although it was recognized that deposition rate would be reduced.

Run 100 was made for 50 hours at 1500°C with a 12 inch long 3 x 6 inch box and flat walls. Deposits about 1/8 inch thick were of uneven thickness and delaminated. Metal content was about 14 percent.

Run 101 was made at 1400°C with other furnace conditions and mandrel design the same as for Run 100. The deposition rate was very low, about 0.5 mils/hr. The deposited material was delaminated.

Run 102 was made at 1500°C using hafnium for the first time in this program. Growth data reported in Reference 6 suggested that growth of HfC/PG might be less than that of ZrC/PG, and might also be less with high hafnium content. Increased chlorine flow was used on Run 102 to raise metal content to an average of 35 wt. percent. A 10 hour run depositing pure PG preceeded the 40 hour pyrocarbide deposition. The PG precoat was intended to stabilize the mandrel and resist bowing caused by growth of the HfC/PG. The deposits within the 3 x 6 x 12 inch long box were badly delaminated.

e.   Runs 103 thru 105

The last three furnace runs were made with reduced mandrel sizes which were just large enough to make washers for a nozzle with a 1.5 inch throat diameter required for the objectives of the program redirection. The smaller mandrels had a smaller flow cross-section which was expected to provide higher deposition rates for the same flow rates. Hafnium was again used on Run 103. A temperature of 1600°C was used on this and remaining runs since it provided high metal content with fair deposition rates. A 5 x 5 x 10 inch long mandrel box was used on Run 103. All flow rates were doubled, except the argon tip flow, in order to increase deposition rates. A 20 hour run was made. The deposit was of good appearance except for 1 delamination in the center. Metal content was about 40 percent. Deposition rate was 5 mils/hr.

Run 104 was made with zirconium. Flow rates were increased almost two-fold. Two mandrel boxes, 5-1/2 inches long, with 2 x 5 inch cross-section were used. The deposited material was 0.20 inch thick, but was badly delaminated. Metal content was about 40 percent. The deposition rate was high, about 8 mils/hr.

Run 105 was made with similar conditions to Run 104 except that the mandrel box cross-section was increased to 2-1/2 x 5 inch and hafnium was used instead of zirconium. The metal content in the 1/4 inch thick material deposited during a 26.5 hour run was 65 percent. Deposition rate was 9.4 mils/hr. A 3/8 inch thick deposit was formed on the lid but was bowed and delaminated. It was concluded from this run that delaminations in high hafnium content material were not significantly less than in zirconium pyrocarbide.

After completion of Run 105, Raytheon made a run with their company funding to deposit HfC/PG plates on rigid mandrels made from 1 inch thick graphite. Several plates with an O.D. of 3.9 inches were produced with only slight bow. Original thicknesses were about 0.250 inch, but most of the plates delaminated during machining, indicating that the flat plates contained very high residual stresses.

f.   Conclusions

The following conclusions were drawn regarding the fabrication of flat plate of pyrocarbides.

(1)   Production of flat pyrocarbide plates is much more difficult than production of flat pyrolytic graphite.

(2)   Hafnium pyrocarbide plate has tendencies to bow and delaminate which are not significantly less severe than similar behavior of zirconium pyrocarbide.

(3)   The mandrel design with best promise of providing pyrocarbide plate is one perpendicular to the flow direction.   The thickest pyrocarbide plate deposited without delaminations was deposited on the lid of Run 96. This plate was bowed, but contained 11.2 wt. percent zirconium compared to only 1.5 percent on the sides of the box. Fabrication of washer nozzles, using bowed plates, is not difficult and such an approach was used in the washer nozzle tested under this program.

(4)   The injector designed by Marquardt was largely successful in eliminating plugging but did not completely eliminate the problem of plugging on long runs.

64

2. DESIGN AND ANALYSIS

A pyrolytic graphite washer nozzle shown in Figure 34 was designed and fabricated by AFRPL with a throat diameter of 1.47 inch to meet the nozzle configuration specified by the program redirection. A total of 0.100 inch axial gap was provided between the PG washers to allow thermal expansion.

A nozzle was fabricated by Marquardt with pyrocarbide washers in the throat as shown in Figure 35. The ZrC/PG washer was made from the plate deposited on the lid on Run 96. It was machined flat on one face and mated to a concave PG plate on the other face. The HfC/PG washers were made from material provided by Raytheon after the completion of Run 105.

The pyrocarbide washers were assembled in a nozzle similar to that shown in Figure 34.

3. TEST FIRING EVALUATION

The PG washer nozzle, made of Pfizer pyrolytic graphite, was tested for 73 seconds, during which the chamber pressure dropped from 562 psig to 225 psig. The nozzle eroded badly, as shown in Figure 36. The rough scalloped surface of the nozzle indicated that erosion was by mechanical spalling rather than by chemical erosion. The reason for this mechanical spalling is not known, but it is speculated that residual stresses might have played a role.

The pyrocarbide washer nozzle was tested at AFRPL with N_2O_4/MMH at an initial chamber pressure of 508 psig and a mixture ration of 1.82. The C* efficiency was 86.8 percent. The pyrocarbide washer nozzle was tested for 24 seconds, during which the chamber pressure dropped from 508 psig to 327 psig. The HfC/PG washers delaminated and cracked, with failure apparently caused by residual stresses. There were gaps between the pieces of HfC/PG washers remaining. Portions of the HfC/PG washers were covered with deposits which had apparently been molten, as shown in Figure 37. Some of the deposits were tan or white, and had the appearance of an oxide. Other deposits were metallic and shiny with a silver color.

The combustion gas in recirculation zones between the partially removed HfC/PG washers could have exceeded 5250°F, the approximate melting point of HfO_2.

The zirconium pyrocarbide washer had eroded in a manner very similar to the pyrolytic graphite washers. There was no evidence of dry or molten oxide having formed. It seems likely that surface spalling of the washer was so rapid that a significant oxide layer could not form.
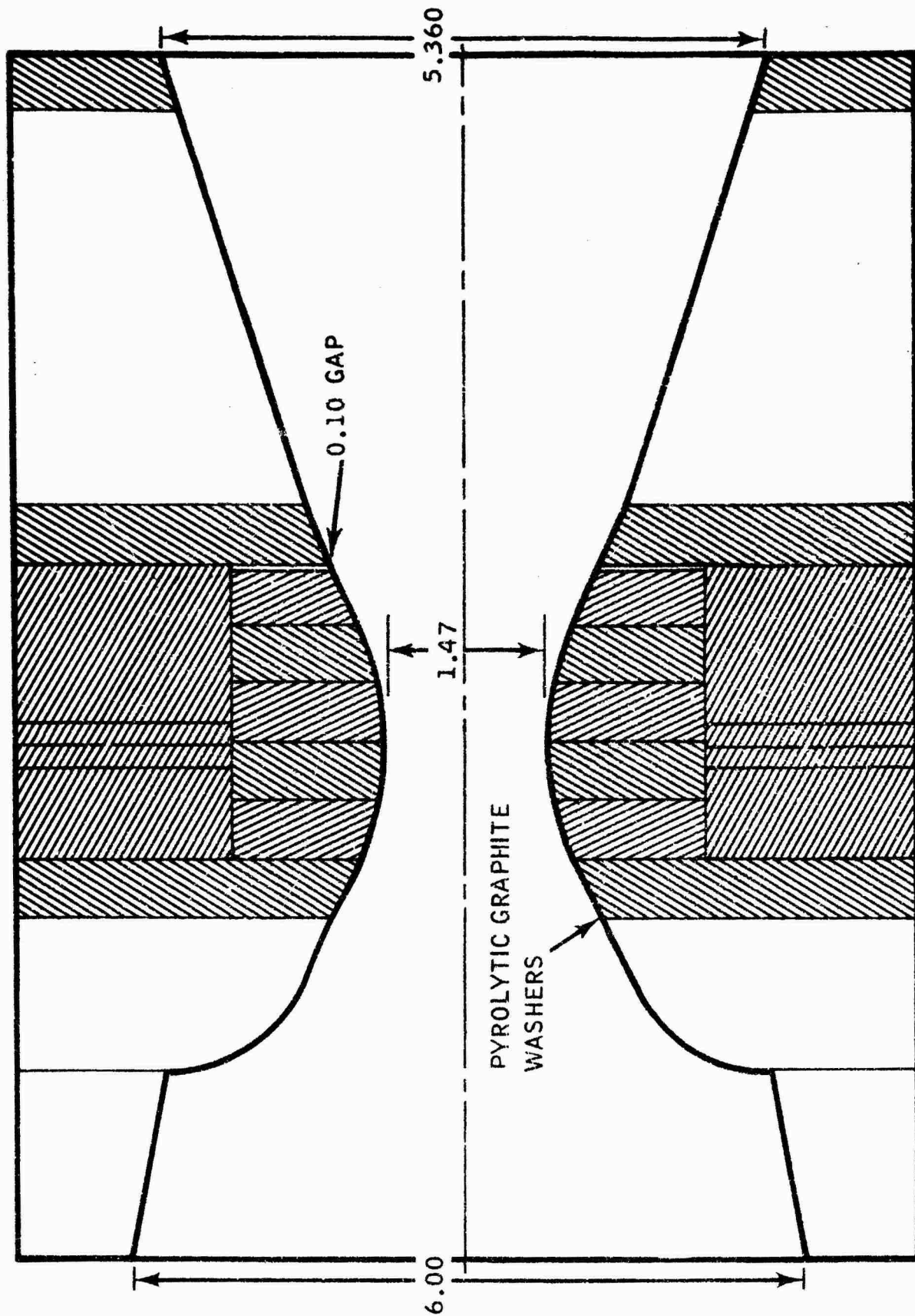
5.360

0.10 GAP

1.47

PYROLYTIC GRAPHITE
WASHERS

6.00

FIGURE 34. PYROLYTIC GRAPHITE WASHER NOZZLE DESIGN

4.197 DIA.

3.197 DIA.

1.47 DIA.

PFIZER PG (0.5 IN.)

SUPER TEMP PG (.25 IN.)

14% HfC/PG (.016 IN.)

14% HfC/PG (0.22 IN.)

11% ZrC/PG $\left(\begin{array}{l}\text{0.415 IN. INSIDE}\\ \text{0.295 IN. OUTSIDE}\end{array}\right)$
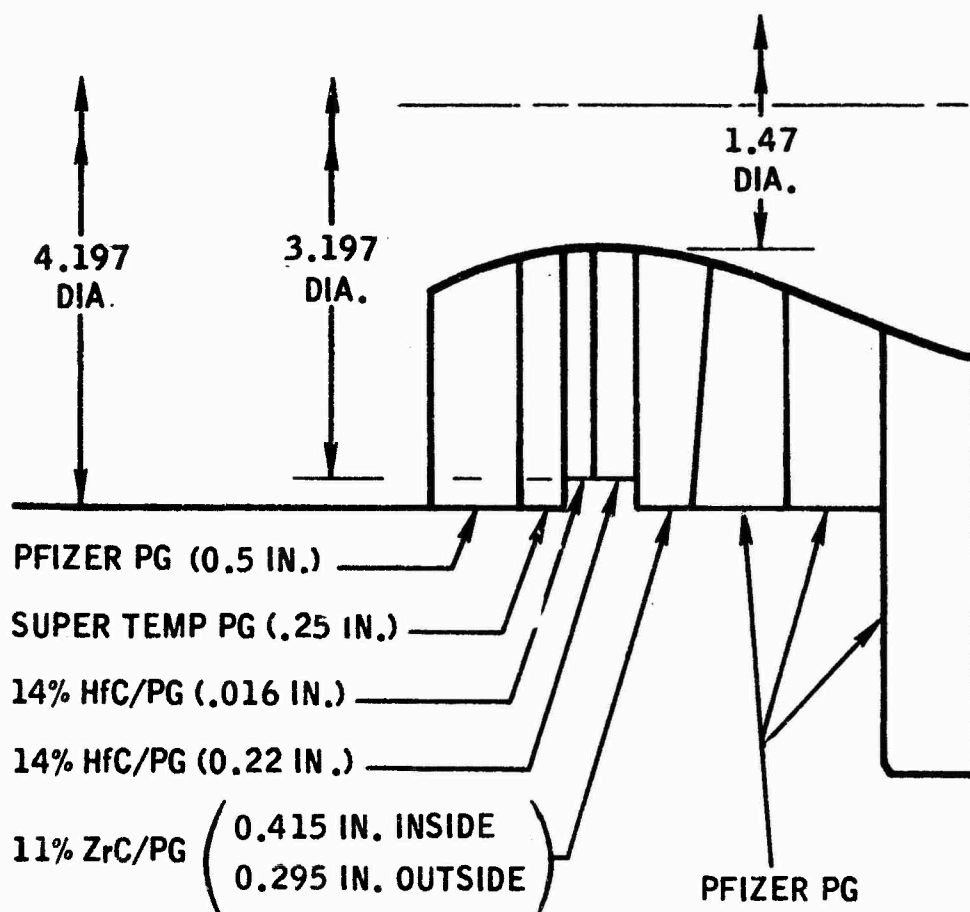
PFIZER PG

FIGURE 35. PYROCARBIDE WASHER DESIGN

FIGURE 26. PYROLYTIC GRAPHITE WASHER NOZZLE AFTER TEST

FIGURE 37. HfC/PG WASHER AFTER TEST

The following conclusions were drawn from the washer nozzle test firings:

(a)   Erosion of the nozzles was primarily mechanical. The reason for
        the severe mechanical spalling is not known.

(b)   There was some evidence that molten HfO_2 was formed on the
        HfC/PG washers and adhered rather well in recirculation zones.
        Failure of the HfC/PG washers due to delaminations was more
        severe than that of the ZrC/PG washer. This was probably due to
        the presence of larger residual stresses in the flat HfC/PG deposited
        on rigid mandrels, as compared to the bowed ZrC/PG plate.

(c)   The throat erosion of the pyrocarbide nozzle was about the same
        as erosion of the pyrolytic graphite washer nozzle.

(d)   Deposition rate increased with increasing furnace temperature as shown
        in Figure 38 .

(e)   Wt. percent metal decreased with increasing furnace temperature,
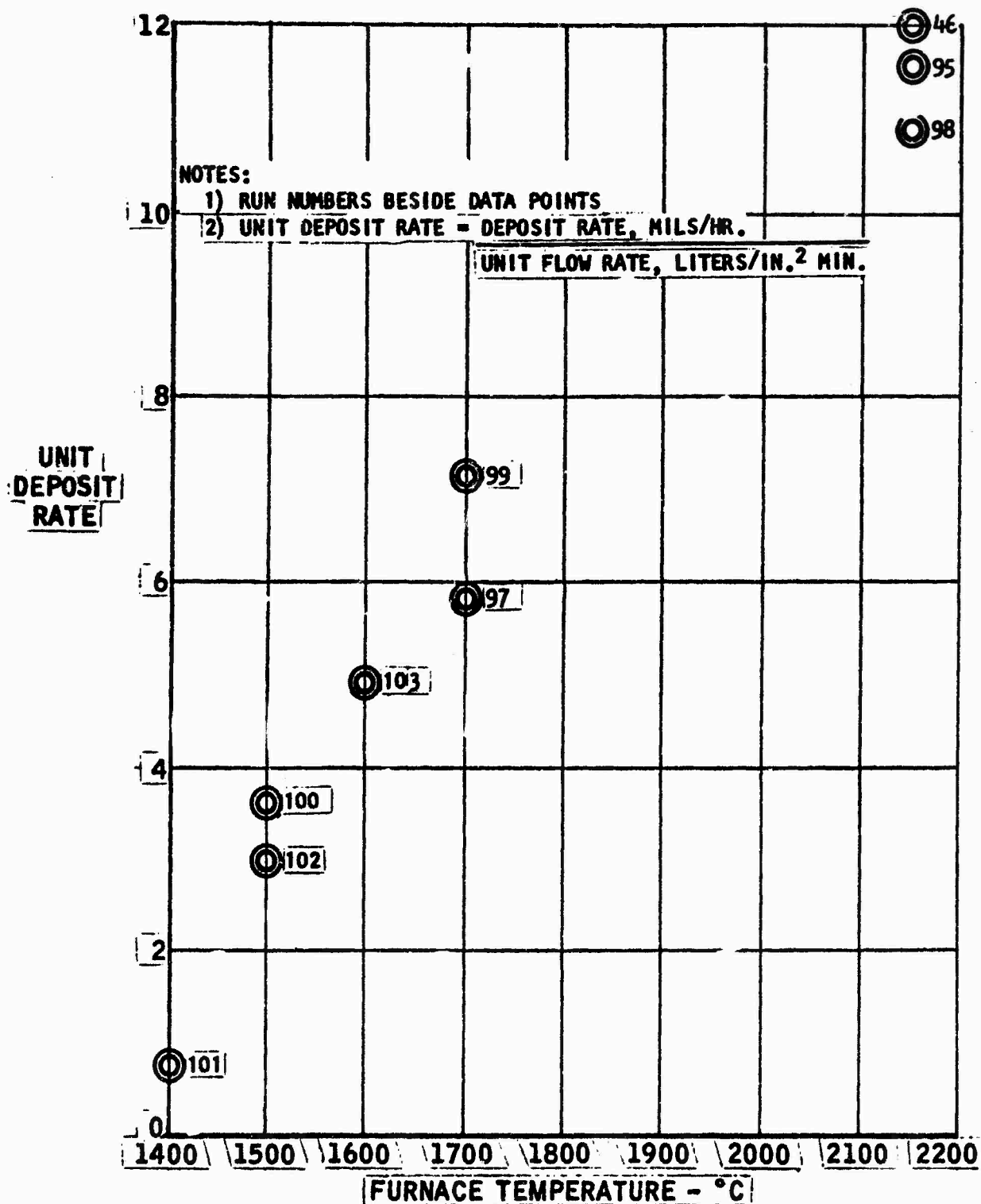   as shown in Figure 39 .
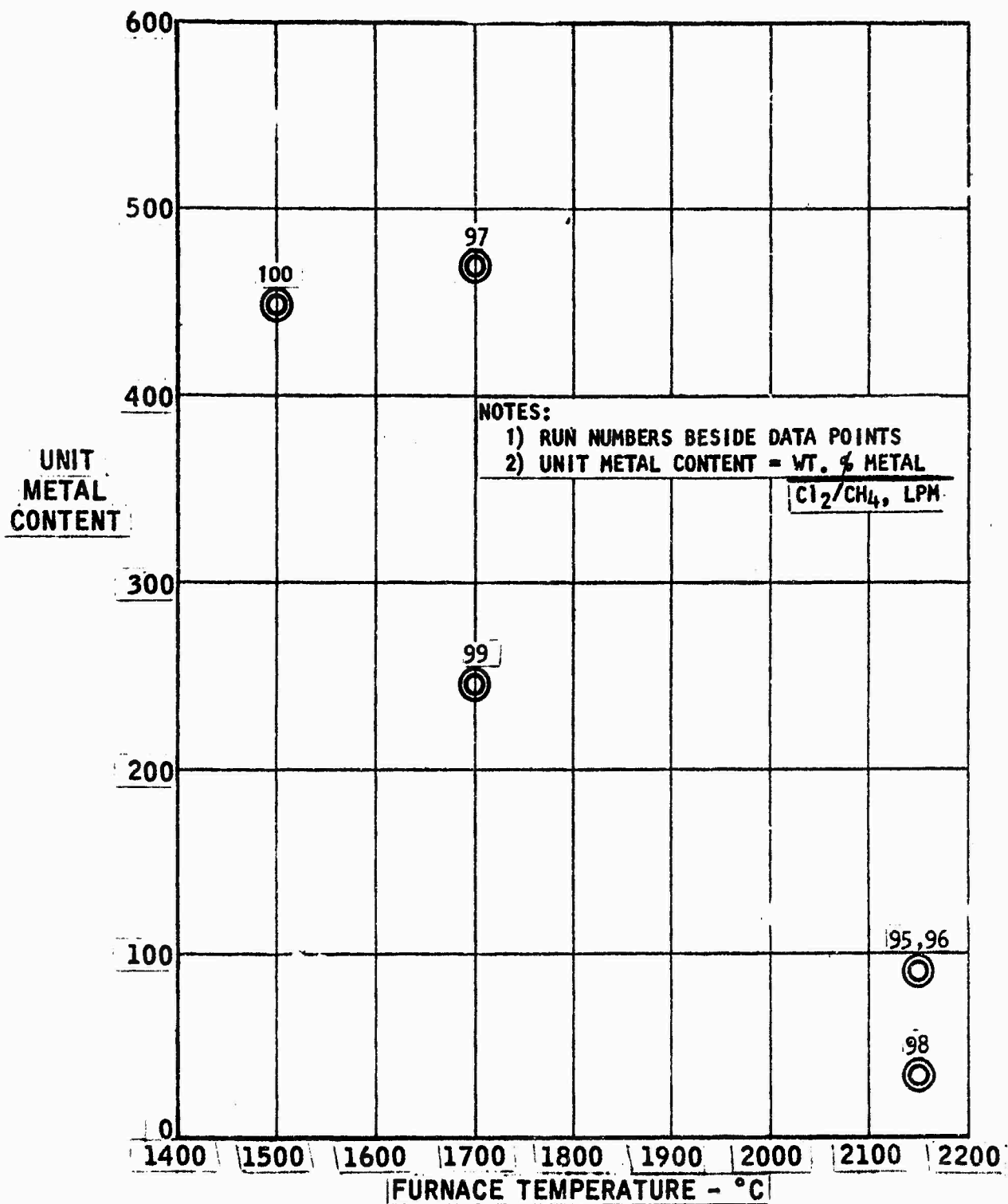
FIGURE 38. UNIT DEPOSIT RATE - VS - FURNACE TEMPERATURE

FIGURE 39. UNIT METAL CONTENT - VS - FURNACE TEMPERATURE

72

SECTION X

CONCLUSIONS

The results of this study lead to the following conclusions:

1. A segmented nozzle insert using pre-oxidized boride alloys such as Man Lab's Material VIII (18,10) has demonstrated excellent erosion resistance as an uncooled nozzle material for N_2O_4/Amine propellants.

2. The use of pre-oxidation and segmentation of Material VIII (18,10), together with thermal stress analysis design criteria, was successful in providing a nozzle insert design which endured peak thermal stresses without failure.

3. The pyrolytic graphite spring design used for containment of segmented inserts was not completely successful. Design modifications or optimized spring thickness might eliminate the problem of cracking and displacement encountered by the springs.

4. Hafnium pyrographite and zirconium pyrographite washers were not successful in reducing erosion below that experienced on pyrolytic graphite washers due largely to mechanical spalling rather than oxidation.

5. Fabrication methods for producing large pyrocarbide washers could not be established during this program. Deposition on mandrels perpendicular to gas flow was the method with most indication of promise.

6. The injector designed by Marquardt was largely successful in preventing injector plugging as a restriction on furnace run duration for fabrication of pyrocarbide washers. Improved designs based on the same principle could be expected to be even more successful in preventing injector plugging.

7. Dendritic growths during deposition of pyrocarbide coatings on Carbitex occurred on two furnace runs, preventing fabrication and test firings of this type of nozzle. Such growths could probably be eliminated without much difficulty.

8. A pyrolytic graphite coating on a Carbitex nozzle demonstrated excellent adhesion and low erosion rates, although not low enough for the original goals of this program.

73

SECTION XI

RECOMMENDATIONS

1. Additional test firings of a number of segmented pre-oxidized boride inserts should be performed over a range of chamber pressures to determine operational limits of this new nozzle design concept. Thermal stress analysis and heat flux measurements should be performed to correlate the test results.

2. Fabrication and test firings of zirconium pyrocarbide and hafnium pyrocarbide coated nozzles using Carbitex and PYROBOND substrates should be completed. The superior performance of the pyrolytic graphite coated Carbitex nozzle, compared to the pyrolytic graphite washers, might be further enhanced by oxidation resistance of pyrocarbide coatings.

SECTION XII

REFERENCES

1. Winter, J.M. and Peterson, D.A., "Development of Improved Throat Inserts for Ablative Rocket Engines", NASA TND-4964, July 1969.

2. Kubaschewski and Hopkins, "Oxidation of Metals and Alloys,"p. 92

3. Armour, W.H. et al, "Evaluation of Materials for Potential Application as Uncooled Liquid Rocket Hard Throat Inserts", Philco-Ford Corp., SRS Publication No. TN-70-004, January 1970.

4. Timoshenko and Goodier, "Theory of Elasticity".

5. Marquardt Report 6142, "Pyrolytic Refractory Materials for Spacecraft Thrust Chambers - Composite Fabrication Investigation", NAS 7-555, 4 October 1968.

6. Marquardt Report 6115, "Pyrolytic Refractory Materials for Spacecraft Thrust Chambers", NAS 7-373, 15 December 1966.